Polyol Recognition by a Steroid-Capped Porphyrin. Enhancement and Modulation of Misfit Guest Binding by Added Water or Methanol

Richard P. Bonar-Law* and Jeremy K. M. Sanders*

Contribution from the Cambridge Centre for Molecular Recognition, University Chemical Laboratory, Lensfield Road, Cambridge CB2 1EW, U.K.

Received May 11, 1994[⊗]

Abstract: A spacious semisynthetic receptor composed of a zinc porphyrin bridged by a steroidal diol is shown to complex alcohols and polyols in nonpolar solvents by a combination of Lewis acid coordination and hydrogen bonding, with negative free energies ranging from < 0 to > 45 kJ/mol (equilibrium constants ranging from $K < 1$ to $K > 10^8$ L/mol). The physical basis of polyol recognition is discussed in terms of the binding properties of the floor (zinc porphyrin) and roof (steroidal diol) components of the receptor. Lewis acid-induced polarization of the OH bond of a bound alcohol is found to promote hydrogen-bonded association of a second molecule of alcohol and to enhance cyclization of metal-bound diols. Organic-soluble pyranoside derivatives are complexed by the receptor more strongly than by the roof or floor components alone. A semiquantitative two-point binding model is developed to understand binding energetics and solvent effects. An inherent "stickiness order" for pyranosides based on the extent of intramolecular hydrogen bonding is proposed and used to rationalize binding selectivities. Following the observation that two or more molecules of an alcohol or small diol can bind cooperatively inside the receptor cavity, addition of water and methanol is shown to increase and modulate pyranoside binding by filling in the gaps between the receptor and a misfit ligand. A quantitative analysis of binding enhancements is presented, and parallels are drawn between synthetic receptors operating in nonpolar solution and natural receptors operating in water.

Introduction

The design of synthetic receptors is a fast-growing area of supramolecular chemistry,[1] the aim being to understand and use intermolecular forces to produce devices such as catalysts and sensors.[2] Since metalloporphyrins mediate ligand and electron transfer and can catalyze several types of reactions[3] porphyrins are attractive components for making synthetic receptors. Numerous strapped, capped, crowned, and otherwise elaborated porphyrins have been prepared,[4] mainly for studies of small molecule binding e.g. CO vs O_2 or as biomimetic catalysts for monooxygenase chemistry. However most porphyrin receptors have largely unfunctionalized binding sites,[5] recognizing their substrates by geometrically relatively nonspecific forces such as van der Waals, hydrophobic, and $\pi-\pi$ interactions, and few are spacious enough to accommodate even moderately sized species. Our approach has been to design large, functionalized porphyrin-based receptors; the arrows representing functional

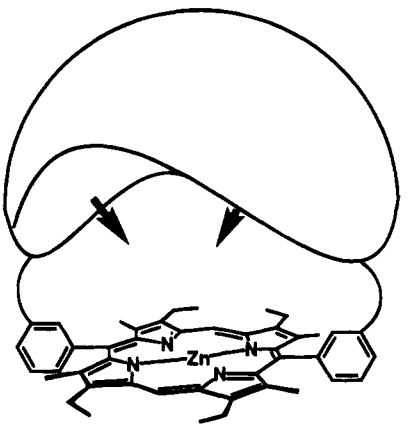

groups able to clasp and recognize a substrate. Receptor Zn1[6] positions a pair of chiral convergent hydroxyl groups over the

[⊗] Abstract published in *Advance ACS Abstracts*, December 1, 1994.

(1) (a) Webb, T. H.; Wilcox, C. S. *Chem. Soc. Rev.* **1993**, 383. (b) Diederich, F. *Cyclophanes*; Royal Society of Chemistry: London, 1991.

(2) Lehn, J. M. *Angew. Chem., Int. Ed. Engl.* **1990**, *29*, 1304.

(3) See, for example: (a) Bartley, D. W.; Kodadek, T. J. *Tetrahedron Lett.* **1990**, *31*, 6303. (b) Konishi, K.; Makita, K.; Aida, T.; Inoue, S. *J. Chem. Soc., Chem. Commun.* **1988**, 643. (c) Aoyama, Y.; Tanaka, Y.; Yoshida, Y.; Toi, H.; Ogoshi, H. *J. Organomet. Chem.* **1987**, *329*, 251.

(4) The following is a selection of structurally diverse capped porphyrin receptors and biomimetics: (a) Blasco, A.; Garcia, B.; Bruice, T. C. *J. Org. Chem.* **1993**, *58*, 5738. (b) Collman, J. P.; Lee, V. J.; Zhang, X.; Ibers, J. A.; Brauman, J. I. *J. Am. Chem. Soc.* **1993**, *115*, 3834. (c) Naruta, Y.; Ishihara, N.; Tani, F.; Maruyama, K. *Bull. Chem. Soc. Jpn.* **1993**, *115*, 3834. (d) Katsuaki, K.; Oda, K. I.; Nishida, K.; Aida, T.; Inoue, S. *J. Am. Chem. Soc.* **1992**, *114*, 1313. (e) Imai, H.; Nakagawa, S.; Kyuno, E. *J. Am. Chem. Soc.* **1992**, *114*, 6719. (f) Wytko, J. A.; Graf, E.; Weiss, J. *J. Org. Chem.* **1992**, *57*, 1015. (g) Collman, J. P.; Zhang, X.; Lee, V. J.; Brauman, J. I. *J. Chem. Soc., Chem. Commun.* **1992**, *1647*. (h) Slobodkin, G.; Fan, E.; Hamilton, A. D. *New J. Chem.* **1992**, *16*, 643. (i) Groves, J. T.; Viski, P. *J. Org. Chem.* **1990**, *55*, 3628. (j) Kuroda, Y.; Hiroshige, T.; Ogoshi, H. *J. Chem. Soc., Chem. Commun.* **1990**, 1594. (k) Benson, D. R.; Valentekovich, R.; Diederich, F. *Angew. Chem., Int. Ed. Engl.* **1990**, *29*, 191. (l) Collman, J. P.; Zhang, X.; Hembre, R. T.; Brauman, J. I. *J. Am. Chem. Soc.* **1990**, *112*, 5356. (m) O'Malley, S.; Kodadek, T. *J. Am. Chem. Soc.* **1989**, *111*, 9116. (n) Wijeskera, T. P.; Paine, J. B.; Dolphin, D. *J. Org. Chem.* **1988**, *53*, 1345. (o) Lindsey, J. S.; Delaney, J. K.; Mauzerall, D. C.; Linschitz, H. *J. Am. Chem. Soc.* **1988**, *110*, 3601. (p) Simonis, U.; Walker, F. A.; Lani, Lee, P.; Hanquet, B.; Meyrhoff, D. J.; Scheidt, W. R. *J. Am. Chem. Soc.* **1987**, *109*, 2659. (q) Renaud, J.-P.; Battioni, P.; Mansuy, D. *New J. Chem.* **1987**, 279. (r) Momenteau, M. *Pure Appl. Chem.* **1986**, *58*, 1493. (s) Traylor, T. G.; Tsuchiya, S.; Campbell, D.; Mitchell, M.; Stynes, D.; Koga, N. *J. Am. Chem. Soc.* **1985**, *107*, 604. (t) Tsuchiya, S. *Inorg. Chem.* **1985**, *24*, 4452. (u) Boitrel, B.; Lecas, A.; Renko, Z.; Rose, E. *New J. Chem.* **1989**, *13*, 73. (v) Staubli, B.; Fretz, H.; Piantini, U.; Woggon, W.-D. *Helv. Chim. Acta.* **1987**, *70*, 1173. (x) Baldwin, J. E.; Perlmutter, P. in *Topics in Current Chemistry*; Vogtle F., Weber, E., Eds.; Springer-Verlag: New York, 1984, Vol. 121, 181.

(5) For nonmacrocyclic porphyrins bearing peripheral functionality see for example (a) Mizutani, T.; Ema, T.; Tomita, T.; Kuroda, Y.; Ogoshi, H. *J. Chem. Soc., Chem. Commun.* **1993**, 520. (b) Hayashi, T.; Miyahara, T.; Hashizume, N.; Ogoshi, H. *J. Am. Chem. Soc.* **1993**, *115*, 2049. (c) Hayashi, T.; Asai, T.; Hokazano, H.; Ogoshi, H. *J. Am. Chem. Soc.* **1993**, *115*, 12210. (d) Naruta, Y.; Tani, F.; Maruyama, K. *J. Chem. Soc., Chem. Commun.* **1990**, 1378. (e) Breslow, R.; Brown, A. B.; McCullough, R. D.; White, P. W. *J. Am. Chem. Soc.* **1989**, *111*, 4517. (f) Sasaki, T.; Kaiser, E. T. *J. Am. Chem. Soc.* **1989**, *111*, 380. (g) Maillard, P.; Guerguin-Kern, J.-L.; Momenteau, M.; Gaspard, S. *J. Am. Chem. Soc.* **1989**, *111*, 9125. (h) Lindsey, J. S.; Kearney, P.; Duff, R. J.; Tjivikua, P.; Rebek, J. *J. Am. Chem. Soc.* **1988**, *110*, 6575. (i) Aoyama, Y.; Uzawa, J.; Saita, K.; Tanaka, Y.; Toi, H.; Ogoshi, H. *Tetrahedron Lett.* **1988**, *29*, 5271. (j) Reid, C. A.; Scheidt, W. R. *Inorg. Chem.* **1987**, *26*, 3649. (k) Buckingham, D. A.; Gunter, M. J.; Mander, L. N. *J. Am. Chem. Soc.* **1978**, *100*, 2899.

0002-7863/95/1517-0259$09.00/0

porphyrin using a steroidal dilacetone derived from cholic acid, a readily available hydroxylated steroid.[7] **Zn1** represents a readily accessible first generation receptor, not targeted at any particular substrate; subsequent exploration of its binding

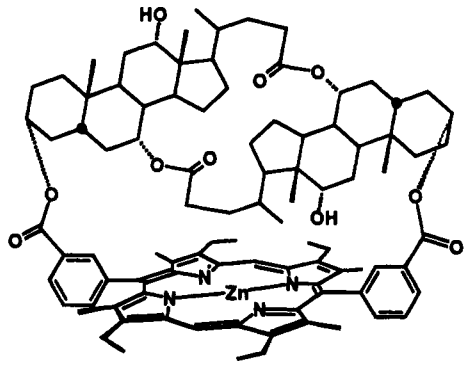

Zn1

properties would then indicate what adjustments might be necessary to fine-tune recognition. Following the pioneering work of Burrows[8] and Davis,[9] we have previously used the rigidity and functionality of cholic acid to create semisynthetic receptors for a variety of substrates including alkaloids and metal ions.[10,11]

Given the importance of oligosaccharides in cellular recognition,[12] the design of receptors for sugars is of much current interest.[13,9c,e] This paper explores the ability of **Zn1** to complex alcohols and organic-soluble pyranoside derivatives by a combination of Lewis acid coordination and hydrogen bonding in nonpolar media. Emphasis is placed on the physical basis of polyol recognition, and a simple model for pyranoside complexation by **Zn1** is proposed. Binding selectivities are discussed in terms of intrinsic receptor selectivity and the competition between ligand inter- and intramolecular hydrogen bonding. It is concluded that while **Zn1** is a moderately effective receptor, it is poorly complementary to pyranosides. Interestingly, this receptor–ligand mismatch could be exploited to enhance and modulate sugar recognition by using water or methanol to fill the gaps between the receptor and poorly fitting ligands. A quantitative treatment of binding enhancements in terms of a system of solvation equilibrium is presented, and the implications of the results for both synthetic and natural receptors are discussed.

Results and Discussion

In order to understand the structural basis for recognition by **Zn1**, it is necessary to understand the properties of its component parts. Porphyrin diester **Zn2** was used as a model for the floor of **Zn1**. Steroidal dilactone diol **3**[6] was used as model for the

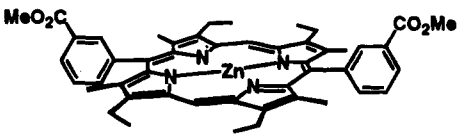

Zn2

roof component of **Zn1**. Molecular models indicate that dilac-

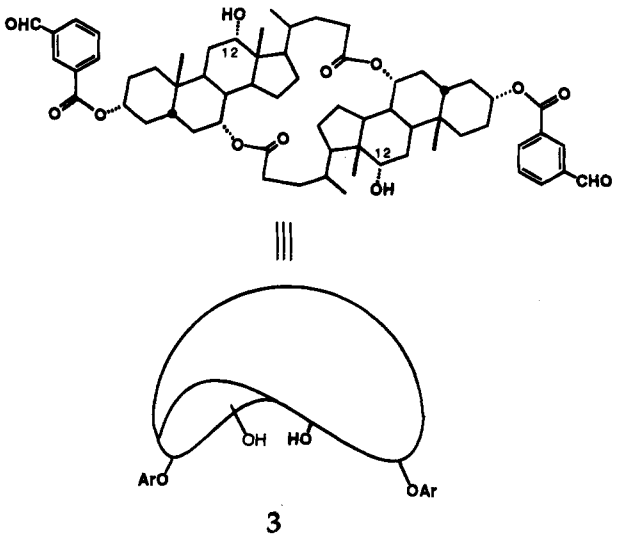

3

tone **3** is cup-shaped with the two hydroxyl groups projecting down and slightly inward. The ability of dilactone **3** to complex alcohol, diol, and pyranoside ligands is first examined, followed by a similar set of binding studies with **Zn2**. Ligand recognition by **Zn1** and its metal-free version H_2**1** is then explored, along with some solution properties of organic-soluble pyranosides relevant to the interpretation of binding results.

Dilactone 3 Binding Alcohols Diols, and Pyranosides. Addition of up to 5 equiv of methanol, propanol, or ethanediol to **3** in $CDCl_3$ produced small downfield shifts (<0.1 ppm) of the 12-O*H* cap hydroxyl doublet (J = 4 Hz) which were essentially linear in ligand concentration. Intermolecular proton exchange between hydroxyl groups was slow enough in acid-free $CHCl_3$ to see all the individual, coupled OH resonances during ^{1}H NMR titrations, the chemical shift of any particular hydroxyl proton being observed as a fast exchange average of its free and bound forms. These observations are consistent with weak unselective binding of alcohols to the secondary hydroxyls of **3**.

In contrast, titration of **3** in $CDCl_3$ with pyranosides **4** to **6**

(6) Synthetic details for **Zn1** will be published elsewhere. The synthesis of a related receptor also employing steroidal dilactone **3** has been communicated; see ref 10c.

(7) Davis, A. P. *Chem. Soc. Rev.* **1993**, 243.

(8) (a) Kinneary, J. F.; Roy, T. M.; Albert, J. S.; Yoon, H.; Wagler, T. R.; Shen, L.; Burrows, C. J. *J. Inclusion Phenom.* **1989**, *7*, 155. (b) Burrows, C. J.; Sauter, R. A. *J. Inclusion Phenom.* **1987**, *5*, 117.

(9) (a) Bonar-Law, R. P.; Davis, A. P. *Tetrahedron* **1993**, *49*, 9829; 9845. (b) Bonar-Law, R. P.; Davis, A. P.; Dorgan, B. J. *Tetrahedron* **1993**, *49*, 9855. (c) Bhattarai, K. M.; Bonar-Law, R. P.; Davis, A. P.; Murray, B. A. *J. Chem. Soc., Chem. Commun.* **1992**, 752. (d) Davis, A. P.; Orchard, M. G.; Slawin, A. M. Z.; Williams, D. J. *J. Chem. Soc., Chem. Commun.* **1991**, 612. (e) Bonar-Law, R. P.; Davis, A. P.; Murray, B. A. *Angew. Chem., Int. Ed. Engl.* **1990**, *12*, 1407.

(10) (a) Bonar-Law, R. P.; Mackay, L. G.; Sanders, J. K. M. *J. Chem. Soc., Chem. Commun.* **1993**, 456. (b) Bonar-Law, R. P.; Sanders, J. K. M. *Tetrahedron Lett.* **1992**, *33*, 2071. (c) Bonar-Law, R. P.; Sanders, J. K. M. *J. Chem. Soc., Chem. Commun.* **1991**, 574.

(11) For other receptors employing steroids, see: (a) Kikuchi, J.; Matsushima, C.; Suehiro, K.; Oda, R.; Murakami, Y. *Chem. Lett.* **1991**, 1807. (b) Shinkai, S.; Nishi, T.; Matsuda, T. *Chem. Lett.* **1991**, 437. (c) Groves, J. T.; Neumann, R. *J. Am. Chem. Soc.* **1989**, *111*, 2900. (d) Guthrie, J. P.; Cossar, J.; Dawson, B. A. *Can. J. Chem.* **1986**, *64*, 2456 and previous papers in this series. (e) McKenna, J.; McKenna, J. M.; Thornthwaite, D. W. *J. Chem. Soc., Chem. Commun.* **1977**, 809.

(12) Sharon, N.; Lis, H. *Sci. Am.* **1993**, 74.

(13) (a) Liu, R.; Still, W. C. *Tetrahedron Lett.* **1993**, *34*, 2573. (b) Savage, P. B.; Gellman, S. H. *J. Am. Chem. Soc.* **1993**, *115*, 10448. (c) Paugain, M.-F.; Morin, G. T.; Smith, B. D. *Tetrahedron Lett.* **1993**, *34*, 7841. (d) Murukami, H.; Nagasaki, T.; Hamachi, I.; Shinkai, S. *Tetrahedron Lett.* **1993**, *34*, 6273. (e) Möhler, L. K.; Czarnik, A. W. *J. Am. Chem. Soc.* **1993**, *115*, 2998. (f) Coteron, J. M.; Vicent, C.; Bosso, C.; Penades, S. *J. Am. Chem. Soc.* **1993**, *116*, 10066. (g) Kikuchi, Y.; Tanaka, Y.; Sutarto, S.; Kobayashi, K.; Toi, H.; Aoyama, Y. *J. Am. Chem. Soc.* **1992**, *114*, 10302. (h) Kobayashi, K.; Asakawa, Y.; Kato, Y.; Aoyama, Y. *J. Am. Chem. Soc.* **1992**, *114*, 10307. (i) Greenspoon, N.; Wachtel, E. *J. Am. Chem. Soc.* **1991**, *113*, 7233. (j) Kikuchi, Y.; Kato, Y.; Tanaka, Y.; Toi, H.; Aoyama, Y. *J. Am. Chem. Soc.* **1991**, *113*, 1349.

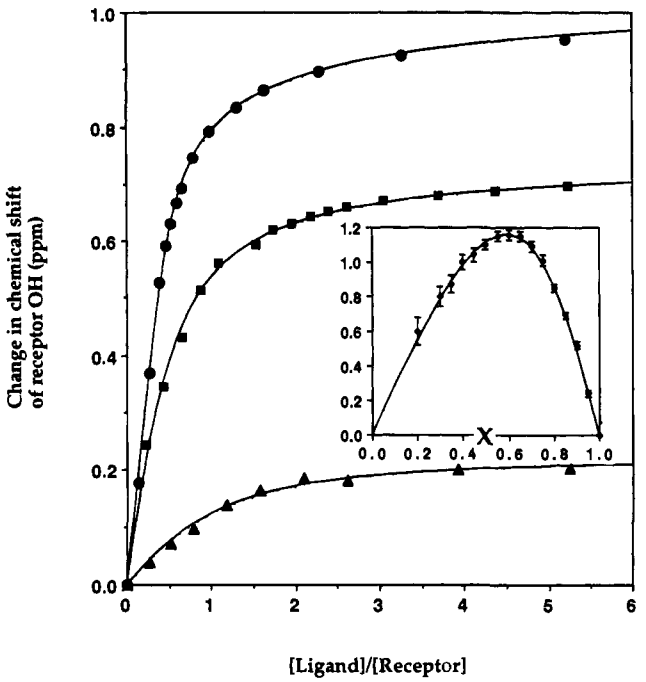

Figure 1. ^{1}H NMR titration data and simulated curve fits for dilactone **3** binding α-mannoside **4** (top), β-glucoside **5** (middle), and α-glucoside **5** (bottom) in $CDCl_3$, monitoring the downfield shift of the dilactone hydroxyl doublet. Insert: Job plot and simulated curve fit for titration of dilactone **3** with β-glucoside **5** in $CDCl_3$. The vertical scale is $[R_o]\ \delta\Delta \times 10^3$ where $[R_o]$ is the total concentration of dilactone **3** (0 to 5 mM) and $\delta\Delta$ is shift in ppm induced in the receptor hydroxyl resonance. The horizontal scale (x) is the mole fraction of **3**, with the total concentration of ligand plus receptor maintained at 5.0 mM. For exclusive formation of a 1:1 or 2:1 complexes, the plot should peak at $x = 0.5$ and $x = 0.67$, respectively.

resulted in large downfield shifts of the cap hydroxyl resonance. The complexation-induced shifts of the 12-O*H* doublet are plotted for three ligands in Figure 1, and the binding energies[14] are given in Table 1. Curve fitting indicated significant deviations from 1:1 stoichiometry at low ligand/receptor ratios. Continuous variation titration with β-glucoside **5** also resulted in an asymmetric Job plot.[15] Simulation analysis of both types of titration data suggested that a second molecule of dilactone binds to the first-formed 1:1 species to form a 2:1 complex. The second binding process was weaker than the first one and was associated with lower limiting downfield shifts of the dilactone hydroxyl resonance. Pyranosides were bound in the order mannose > glucose > galactose for both 1:1 and 1:2 complexes. A sandwich structure is proposed for the termolecular complex, with the sugar effectively enclosed in a hydrophobic shell.[13g] For comparison the simple steroidal diol

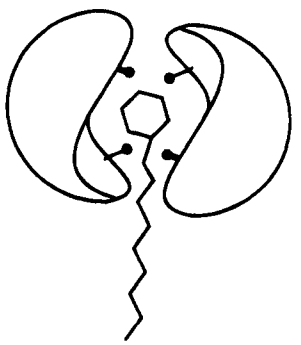

(14) All equilibrium constants in this paper are dimensionless, standard state 1 M.

Table 1. Binding Energies (kJ/mol) of Pyranosides to Zn2 and Dilactone **3**

pyranoside[d]	Zn2 − ΔG^a (CH_2Cl_2)	dilactone **3**	
		$-\Delta G_1{}^b$ ($CDCl_3$)	$-\Delta G_2{}^b$ ($CDCl_3$)
α-D-Mannoside (**4**)	≤11	19(1.0)[c]	16(2.0)
β-D-Glucoside (**5**)	12(1.0)	16(0.8)	13(2.0)
α-δ-Glucoside (**5**)	11(1.5)	15(1.5)	9(2.5)
α-D-Galactoside (**6**)	≤11	9(2.0)	

[a] $\Delta G = -RT \ln(K)$. K determined by UV titration at 295 K. [b] K_1 and K_2 for first and second binding determined by ^{1}H NMR titration in dry solvent at 295 K. [c] Estimated errors. [d] Structures are as follows:

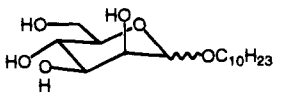

α/β-D-mannoside **4**

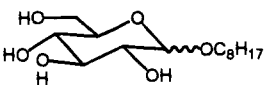

α/β-D-glucoside **5**

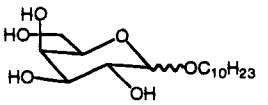

α/β-D-galactoside **6**

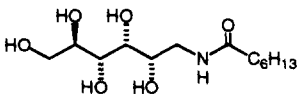

7

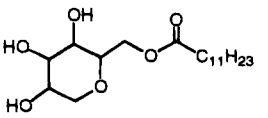

8

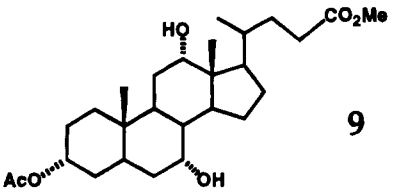

9

9, was also titrated with β-glucoside **5**. Only small downfield shifts (≤0.1 ppm) were seen for both secondary hydroxyls (7-O*H*, $\delta = 1.2$ ppm, $J = 2.5$ Hz and 12-O*H*, $\delta = 1.4$ ppm, $J = 5$ Hz). The binding isotherm for this "receptor" could not be fitted cleanly to any simple scheme due to ligand aggregation; however curve fitting of the part of the isotherm assuming 1:1 stoichiometry gave an upper limit for the binding energy of ≤5 kJ/mol.

Zn2 Binding Alcohols, Diols, and Pyranosides. Equilibrium constants for the ligands in Table 2 were measured by UV-visible titration, using the red shift of the porphyrin Soret and/or Q bands induced on coordination of donor species to the zinc atom.[16] Good isosbestic points were obtained for ether and amine ligands and the binding isotherms were well fitted assuming 1:1 stoichiometry. However alcohol titrations were slightly less isosbestic, and curve fitting implied weak second binding to form 1:2 porphyrin/alcohol adducts. We propose that this is due to hydrogen bonding of a second molecule of alcohol to the polarized hydrogen atom of the initially formed 1:1 complex. An alternative explanation, in which the second

(15) Connors, K. A. *Binding Constants*; Wiley: New York, 1987.

(16) (a) Nardo, J. V.; Dawson, J. H. *Inorg. Chim. Acta* **1986**, *123*, 9. (b) Kroleva, T. A.; Koifman, O. I.; Berezin, B. D. *Koord. Khim.* **1981**, *7*, 1642. (c) Kolling, O. W. *Inorg. Chem.* **1979**, *18*, 1175. (d) Nappa, M.; Valentine, J. S. *J. Am. Chem. Soc.* **1978**, *100*, 5075. (e) Vogel, G. C.; Stahlbush, J. R. *Inorg. Chem.* **1977**, *16*, 950.

Table 2. Binding Energies (kJ/mol) of Alcohols, Diols, Ethers, and Amines to Zn1 and Zn2

	Zn2		Zn1			
ligand	$-\Delta G_1$[a]	$-\Delta G_2$[a]	$-\Delta G_1$	$-\Delta G_2$	$\Delta\Delta G_1$[b]	$\Delta\Delta G_2$
methanol	4.0(0.5)[c]	−1.7(1.0)	2.7(0.7)	4.0(0.8)	+1.3	−5.7
1-propanol	4.0(0.5)	*d*	3.7(0.5)	1.0(0.7)	+0.3	<−1.0
$MeO(CH_2)_2OH$	4.4(0.4)	*d*	4.8(0.3)	*d*	−0.4	
$MeO(CH_2)_2OMe$	2.7(0.3)		1.4(0.1)		+1.3	
diethyl ether	≤0		≤0			
tetrahydrofuran	7.1(0.1)		5.7(0.2)		+1.4	
1,2-ethanediol	≤5.0	*d*	7.3(0.5)	17.0(0.6)	−2.3	<−17
1,3-propanediol	7.3(0.3)	*d*	10.7(0.5)	7.3(1.0)	−3.4	<−7
1,4-butanediol	8.5(0.4)	*d*	10.4(0.1)	*d*	−1.9	
1,5-pentanediol	6.3(0.5)	*d*	5.9(0.4)	*d*	+0.4	
1,8-octanediol	5.4(0.7)	*d*	4.4(1.0)	*d*	+1.0	
1,2-propanediol	5.6(0.4)	4.0(1.0)	8.3(0.4)	9.3(0.5)	−2.7	−5.3
1,2-cyclohexanediol (*trans*)	6.1(0.4)	*d*	9.5(0.1)	*d*	−3.4	
1,3-cyclohexanediol[e]	4.6(0.7)	*d*	8.4(0.4)	*d*	−3.8	
4-phenylpyridine (**10**)	21.9(0.2)		20.0(0.2)		+1.9	
dihydrobenzofuran (**11**)	6.2(0.2)		8.3(0.2)		+2.1	
pyrazole (**12**)	16.5(0.2)		15.6(0.2)		+0.9	
isoxazole (**13**)	1.8(0.2)		0.9(0.2)		+0.9	

[a] $\Delta G = -RT \ln(K)$. K_1 and K_2 for first and second ligand binding measured by UV and/or ^1H NMR titration in CH_2Cl_2 or CD_2Cl_2 at 295 K. [b] $\Delta\Delta G_1 = \Delta G_{Zn1} - \Delta G_{Zn2}$. [c] Estimated errors. [d] K_2 detectable, but too small to determine accurately. [e] A mixture of *cis* and *trans* isomers.

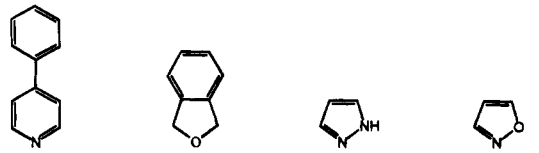

10 **11** **12** **13**

alcohol binds on the opposite side of the porphyrin to form a six-coordinate zinc adduct was rejected for two reasons. (1) Second binding was only observed with ligands containing a free hydroxyl group. (2) The extinction coefficients of the 1:2 complexes were only slightly different from the 1:1 complexes. This is consistent with five-coordinate zinc[17] in the 1:2 complex, which is likely to have an extinction coefficient similar to the 1:1 complex. Kroleva et al. have reported a 1:2 complex between zinc tetraphenylporphyrin (Zn**TPP**) and ethanol in benzene,[16b] although a more recent study of alcohol coordination to Zn**TPP** considered only 1:1 adducts.[16a] Support for a hydrogen-bonded bis-adduct comes from the crystal structure of a zinc porphyrin−methanol solvate,[17b] in which methanol bound to five-coordinate zinc hydrogen bonds to other molecules of methanol. The enhanced acidity of water bound to Lewis acid is well precedented in zinc complexes prepared for model enzyme studies.[18]

α,ω-Alkanediols are partially cyclized by intramolecular hydrogen bonding in nonpolar solvents,[19] with the shortest diols being the most cyclized.[20] Hence coordination to Zn**2** was expected to depend on chain length since when one end of the diol binds, the metal will polarize the OH bond, promoting intramolecular cyclization on the porphyrin and lowering the free energy of the adduct. A variation in ΔG was indeed seen for binding of some α,ω-diols, with maximum binding for diols of medium chain length (Table 2). Ignoring inductive effects, all diols would be expected to have the same binding energy of ca 5.7 kJ/mol; this is derived from the binding energy of a simple alcohol such as methanol or propanol ($-\Delta G$ = 4 kJ/mol) plus a statistical factor of $RT \ln 2$ = 1.7 kJ/mol due to the bidentate nature of the ligand. The same trend was also found for α,ω-diols binding to Zn**TPP** (Table 3). The free energy for zinc-assisted cyclization on the porphyrin, $\Delta G_{cyclize*} = -RT \ln K_{cyclize*}$ was calculated from the thermodynamic cycle below.

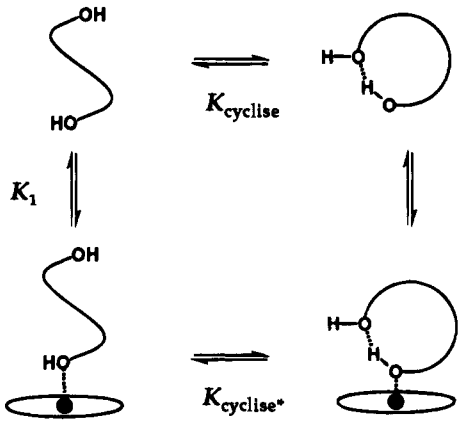

$K_{cyclize*} = (K_{obs}/K_1)(1 + K_{cyclize}) - 1$ where K_{obs} is the experimentally observed equilibrium constant, K_1 is the equilibrium constant for binding of the diol in an open chain form, and $K_{cyclize}$ is the equilibrium constant for intramolecular cyclization of the diol free in solution. K_1 was taken to be twice the value for the first binding of propanol to Zn**TPP** ($K = 2 \times 9.5 = 19$, $-\Delta G_1$ = 7.2 kJ/mol). $K_{cyclize}$ was calculated from the relative intensities of the free and intramolecularly hydrogen-bonded OH stretch bands in the IR spectra of diols in dilute

(17) (a) Schauer, C. K.; Anderson, O. P.; Eaton, S. S.; Eaton, G. R. *Inorg. Chem.* **1985**, *24*, 4082. (b) Barkigia, K.; Berber, M. D.; Fajer, J.; Medforth, C. J.; Renner, M. W.; Smith, K. M. *J. Am. Chem. Soc.* **1990**, *112*, 8851. (c) Glick, M. D.; Cohen, G. H.; Hoard, J. L. *J. Am. Chem. Soc.* **1967**, *89*, 1996.

(18) Kimura, E. *Pure Appl. Chem.* **1993**, *65*, 355.

(19) (a) Aaron, H. S. *Top. Stereochem.* **1979**, *11*, 1. (b) Tichy, M. *Adv. Org. Chem.* **1965**, *5*, 115. (c) Singelenberg, F. A. J.; Van der Maas, J. H. *J. Mol. Struct.* **1991**, *243*, 111. For leading references to alcohol hydrogen bonding in general, see: (d) Beeson, C.; Pham, N.; Shipps, G.; Dix, T. A. *J. Am. Chem. Soc.* **1993**, *115*, 6803.

(20) Busfield, W. K.; Ennis, M. P.; McEwen, I. J. *Spectrochim. Acta* **1973**, *29A*, 1259.

Table 3. Zn**TPP**-Induced Intramolecular Hydrogen Bonding in Acyclic Diols

diol	ΔG_{obs}[a] (kJ/mol)	$\Delta G_{cyclize}$[b]	$\Delta G_{cyclize}$*[c]	$\Delta\Delta G_{cyclize}$[d]	$\Delta H_{cyclize}$[e]
1,2-ethanediol	−5.6(0.6)[f]	−7.8(2.0)	−7.2(2.0)	−1.1	+5
1,3-propanediol	−9.0(0.1)	+0.1(0.3)	−2.7(0.3)	−4.5	−4
1,4-butanediol	−10.4(0.1)	+1.0(0.5)	−4.0(0.3)	−6.7	−13
1,5-pentanediol	−8.1(0.3)	+7.3(2.0)	+1.8(0.7)	−7.2	−8
1,8-octanediol	−7.3(0.5)		+2.1(1.0)		

[a] $\Delta G_{obs} = -RT \ln(K_{obs})$ where K_{obs} is the observed equilibrium constant for diol + Zn**TPP** measured by UV titration in CH_2Cl_2 at 295 K. [b] Energy of intramolecular cyclization of free diol measured by IR in CH_2Cl_2 solution at *RT*. [c] Energy of intramolecular cyclization of diol bound to Zn**TPP**. [d] $\Delta\Delta G_{cyclize} = \Delta G_{cyclize}^* - \Delta G_{cyclize} - 1.7$ kJ/mol. [e] Enthalpy of intramolecular hydrogen bond of free diol in CCl_4 (ref 20). [f] Estimated errors.

CH_2Cl_2 solution.[20] Comparing the free energies for cyclization in solution and on the porphyrin ($\Delta\Delta G$ values in Table 3), coordination to zinc results in a significant stabilization of intramolecularly hydrogen-bonded species. For butanediol and pentanediol this amounts to ~7 kJ/mol or to a ca. 20-fold increase in cyclization. Comparing the $\Delta\Delta G$ values with the enthalpies of cyclization of diols in CCl_4 solution[20] shows that zinc-induced cyclization is most effective if a strong intramolecular hydrogen bond can be formed.[21] Intramolecular hydrogen bonding may also explain increased binding of some of the other oxygen ligands in Table 2. The monomethyl ether of ethanediol binds more strongly to Zn**2** than propanol, and cyclohexane-1,2-diol binds more strongly than cyclohexane-1,3-diol.

Pyranosides were bound unselectively by Zn**2** (Table 1) although equilibrium constants were difficult to measure accurately due to the combination of low ligand solubility, relatively weak binding, and the tendency for pyranoside derivatives to aggregate in nonpolar solvents (see below). Adding pyranosides to free base porphyrin H_2**2** produced no significant change in the UV spectrum. Pyranosides bind to Zn**2** better than expected for single point binding ($-\Delta G_{MeOH} = 4$ kJ/mol plus a statistical factor of $RT \ln 4 = 3.4$ kJ/mol if it is assumed that any of the four hydroxyls can bind to zinc). Part of this extra energy may be due to increased basicity as a result of intramolecular hydrogen bonding. It is also possible that CH or OH-π interactions[22] may contribute. Anchoring one hydroxyl to the zinc atom of Zn**2** would render these weak forces intramolecular and hence more effective.

Zn1 Binding Alcohols and Diols. Alcohol recognition by Zn**1** is best understood by comparison with uncapped porphyrin Zn**2**. The $\Delta\Delta G$ values in Table 2 represent the extra binding due to the superstructure of Zn**1** if ligands bind to the porphyrin floor of Zn**1** and to Zn**2** with the same affinity. To check this assumption binding energies were measured for bulky amine and ether ligands **10** and **11** which models indicate are too big to fit under the steroidal cap of Zn**1**. The average binding energy of these two ligands to Zn**1** was lower than to Zn**2** by $\Delta\Delta G = +2.0$ kJ/mol, which is not far from the statistical result of $RT \ln 2 = +1.7$ kJ/mol expected for a porphyrin of identical electrophilicity to Zn**2**, but blocked on one face.

Likewise, comparison of the binding energies of small ligands **12** and **13** gave an estimate of the strength of inside binding, since models suggest that these ligands should bind without

(21) While we have no independent evidence that diols are in fact more cyclized when coordinated to a porphyrin, the increased basicity of cyclized diols does have literature precedent: (a) Kleeberg, H. *J. Mol. Struct.* **1988**, *177*, 157. (b) Kleeberg, H.; Klein, D.; Luck, W. A. P. *J. Phys. Chem.* **1987**, *91*, 3200.

(22) Kobayashi, K.; Asakawa, Y.; Kikuchi, Y.; Toi, H.; Aoyama, Y. *J. Am. Chem. Soc.* **1993**, *115*, 2648.

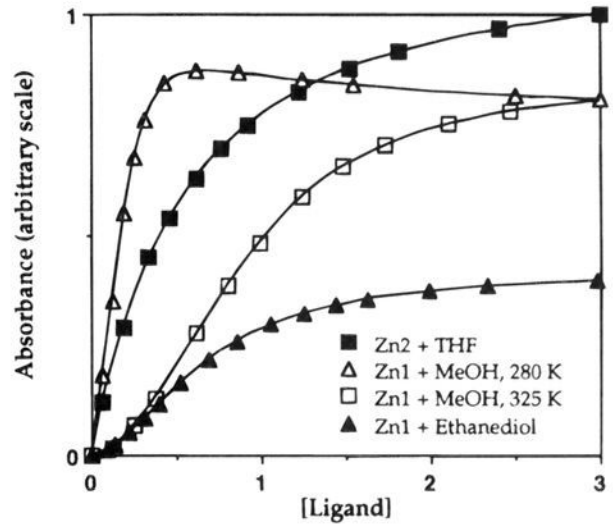

Figure 2. Typical UV titration isotherms showing monophasic, biphasic, and triphasic behavior. Titration of Zn**2** with THF in CH_2Cl_2 to form a 1:1 complex (concentration scale from 0 to 300 mM), titration of Zn**1** with methanol in CCl_4 at two different temperatures forming a mixture of 1:1, 1:2, and 1:3 complexes (concentration scale from 0 to 300 mM) and titration of Zn**1** with ethanediol in CH_2Cl_2 to form a mixture of 1:1 and 1:2 complexes (concentration scale from 0 to 30 mM).

hindrance to both sides of the porphyrin of Zn**1**. The $\Delta\Delta G$ value of +0.9 kJ/mol for both ligands, despite a difference in absolute binding energies of 15 kJ/mol (Table 2), implies that, in CH_2Cl_2, binding under the cap is slightly unfavorable relative to Zn**2**. In the following discussion it will be assumed for simplicity that for weakly binding ligands the intrinsic electrophilicities of both faces of Zn**1** are the same as Zn**2**, and hence the values for $\Delta\Delta G_1$ in Table 2 underestimate the "true" selectivity by ~1 kJ/mol for small ligands (probably due to solvation effects) and ~2 kJ/mol for large ligands (due to the statistical factor). For strongly binding ligands these small energy corrections will be ignored.

The first binding of methanol to Zn**1** is unexceptional (Table 2). However the second binding is enhanced relative to Zn**2** by 5.7 kJ/mol implying that while the hydroxyl groups of Zn**1** are too far from the porphyrin floor to be able to hydrogen bond directly to a zinc-bound alcohol, insertion of a second alcohol molecule completes a chain of hydrogen bonds from floor to roof as shown below. In CCl_4 or cyclohexane, triphasic binding

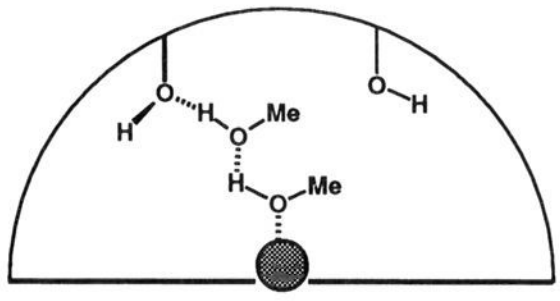

isotherms were obtained (Figure 2) needing a further equilibrium constant to fit the data. At 295 K in CCl_4 the stepwise equilibrium constants for Zn**1** binding one, two, and three molecules of methanol were 15(±8), 40(±15), and 40(±25). As a control experiment, titration of the free base porphyrins H_2**1** and H_2**2** over the same concentration range with methanol in CH_2Cl_2 or CCl_4 produced no significant change in the UV chromophores, demonstrating that a genuine intermolecular association process was being monitored, and not a small red shift due to a change in bulk solvent polarity.

Alcohols aggregate in a cooperative manner since hydrogen-bonded dimers are both more acidic (ROH−O*H*R) and more basic (R*O*H−OHR) than the monomeric alcohol.[23−25] By binding to both ends of an OH−OH chain, an enveloping host like Zn**1** is able to take advantage of the inherent polarization

Table 4. Binding Energies (kJ/mol) of Monosaccharides to Zn1 and (NH_2)**1**

ligand	Zn**1** $-\Delta G^a$ (CH_2Cl_2)	$(NH)_2$**1** $-\Delta G$ (CH_2Cl_2)	$-\Delta G$ ($CHCl_3$)
β-D-mannoside (**4**)	21.0(0.2)[b]		
α-D-mannoside (**4**)	21.7(0.2)	22.0(0.4)	25.3(0.7)
β-D-glucoside (**5**)	17.9(0.2)	16.3(0.3)	20.3(0.5)
α-D-glucoside (**5**)	16.7(0.3)	14.5(0.5)	18.3(0.5)
α-L-glucoside (**5**)	13.6(0.6)		
β-D-galactoside (**6**)	13.0(0.5)		
α-D-galactoside (**6**)	15.2(0.2)		
pentaol **7**	23.7(0.2)[c]		
triol **8**	19.0(0.2)		

[a] $\Delta G = -RT\ln(K)$. K determined by UV and/or ^{1}H NMR titration in dry solvent at 295 K. [b] Estimated errors. [c] K measured in $CHCl_3$ for this ligand.

of hydrogen bonded systems without having to break any intramolecular hydrogen bonds.[26] Zn**1** could be thus be regarded as a receptor for short alcohol oligomers.[27]

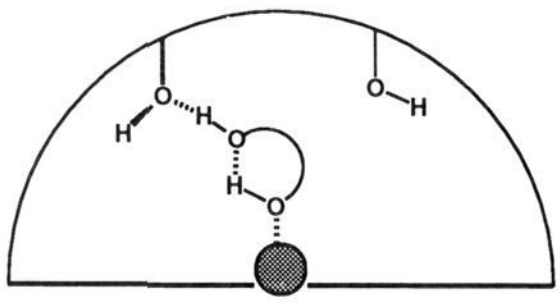

The first binding of some small diols to Zn**1** may be enhanced relative to Zn**2** because the acidic free hydroxyl proton of an intramolecularly hydrogen-bonded diol can hydrogen bond to the cap hydroxyls. Larger diols are bound less well as intramolecular cyclization becomes less favorable and they become too big to fit under the cap. The second binding of the small diols to Zn**1** is remarkably favorable, with a selectivity $\Delta\Delta G_2 \approx 17$ kJ/mol for ethanediol. Double binding of this ligand to Zn**1** is a highly cooperative process, as shown by the pronounced sigmoidal curvature of the binding isotherm (Figure 2); a typical 1:1 binding curve is also plotted for comparison. A Hill plot[15] (not shown) of the ethanediol data is curved, with a slope at low ligand concentration approaching 1 and a slope at high ligand concentration of 1.99, supporting the sequential formation of 1:1 (slope = 1) and 1:2 (slope = 2) complexes. The exceptionally large ΔG_2 for ethanediol appears to be a consequence of unused hydrogen bonding potential due to "free ends" in the initial 1:1 complex which, in conjunction with the small size of this ligand, favors formation of a multiply hydrogen bonded network under the cap.

Zn1 and $H_2$1 Binding Pyranosides. Binding energies are given in Table 4. Shifts in the receptor resonances were monitored during ^{1}H NMR titrations, since the pyranoside resonances were generally broad or unobservable at room temperature in CD_2Cl_2 or $CDCl_3$ due to intermediate exchange on the chemical shift timescale. The 12-O*H* doublet moved rapidly downfield as hydrogen bonding progressed before the signal became too broad to follow. The association was strong enough in dry CCl_4 at room temperature ($K = 1.6 \times 10^6$) to produce slow exchange signals for ligand bound inside the cavity when less than 1 equiv of α-mannoside **4** was added to Zn**1**, with some ligand resonances appearing up to 2.5 ppm upfield of TMS due to the porphyrin ring current. The ligands all induced quite different patterns of shifting in both Zn**1** and H_2**1**, which suggests that each ligand is bound in a different orientation.

Addition of pyranosides to Zn**1** in CH_2Cl_2 solution produced a striking color change from pink to yellow-green due to a ~6 nm red shift of the Soret band, allowing convenient analysis by UV titration. Addition of pyranosides to the free base porphyrin H_2**1** in CH_2Cl_2 produced a much smaller change in the UV spectrum, with a ~1 nm shift of the Soret. Binding isotherms for both H_2**1** and Zn**1** fitted 1:1 stoichiometry well; UV and NMR results agreed within experimental error.

The 6 nm red shift of the Soret band of Zn**1** is similar to the red shift produced by a strongly binding alcohol or ether, implying that sugar ligands coordinate to the zinc atom. The much smaller red shift seen for H_2**1** is attributed to a small complexation-induced conformational change of the porphyrin chromophore rather than coordination to the porphyrin, since no significant shift of the porphyrin NH protons, the most likely hydrogen bonding sites, was observed by NMR.

Pyranosides were bound in the general order mannose > glucose > galactose, with a difference in energy between the strongest and weakest binding ligands of 8.7 kJ/mol, or a factor of 35 in equilibrium constant. Pyranoside anomers were distinguished to the extent of 0.7 kJ/mol (or a binding ratio $K_\alpha/K_\beta = 1.3$) for mannoside **4**, 1.2 kJ/mol ($K_\alpha/K_\beta = 1.6$) for glucoside **5** and 2.2 kJ/mol ($K_\alpha/K_\beta = 2.5$) for galactoside **6**. Moderate enantioselectivity was observed between the L and D enantiomers of α-glucoside **5**, with the natural isomer favored by 3.1 kJ/mol, or a binding ratio of 3.5, corresponding to an enantiomeric excess of 55%.

Binding Selectivity of Zn1. Why are pyranosides bound in the order mannose > glucose > galactose? The extent of intramolecular hydrogen bonding in the ligand will inevitably be a factor if some of the internal hydrogen bonds have to be broken or rearranged on complexation.[26] The less intramolecularly hydrogen bonded a pyranoside is, the "stickier" it will be, where sticky in this context means the ability to form intermolecular hydrogen bonds. Consequently the competition between intra- and intermolecular hydrogen-bonding ability of pyranosides was investigated.

(1) Intramolecular Hydrogen Bonds.[19] In dilute $CDCl_3$ solution the pyranosides displayed sharp, coupled hydroxyl resonances between δ 1.8 and 2.8 ppm, chemical shifts characteristic of intramolecularly hydrogen bonded protons[28,29] (^{1}H NMR assignments are listed in the Experimental Section). The majority of CHOH coupling constants observed were either large (10−11 Hz) or small (0−3 Hz) due to torsion angles of ~180° and ~90° respectively around the CO bonds. This is consistent with a chain of hydrogen bonds which follows the orientation of the hydroxyl groups within the pyranoside.[30] A continuous chain of hydrogen bonds is also expected to be the most enthalpically favorable arrangement, with each bond

(23) (a) Frange, B.; Abboud, J.-L. M.; Benamou, C.; Bellon, L. *J. Org. Chem.* **1982**, *47*, 4553. (b) Pérez-Casas, S.; Moreno-Esparza, R.; Costas, M.; Patterson, D. *J. Chem. Soc. Faraday Trans.* **1991**, *87*, 1745. (c) Brink, G.; Glasser, L. *J. Mol. Struct.* **1986**, *145*, 219. (d) Smith, F. *Aust. J. Chem.* **1977**, *30*, 23; 43. (e) Davis, J. C.; Deb, K. K. *Adv. Magn. Reson.* **1970**, *4*, 201.

(24) Jeffrey, G. A.; Saenger, W. *Hydrogen Bonding in Biological Structures*; Springer-Verlag: New York, 1991.

(25) Newton, M. D. *Acta Crystallogr.* **1983**, *B39*, 104.

(26) (a) Huang, C. Y.; Caball, L. A.; Anslyn, E. V. *J. Am. Chem. Soc.* **1994**, *116*, 2778. (b) Huang, C. Y.; Caball, L. A.; Lynch, V.; Anslyn, E. V. *J. Am. Chem. Soc.* **1992**, *114*, 1900.

(27) Metalloreceptors which bind two molecules of water or methanol in the solid state have been reported: (a) Reichwein, A. M.; Verboom, W.; Harkema, S.; Spek, A. L.; Reinhoudt, D. N. *J. Chem. Soc., Perkin Trans. 2* **1994**, 1167. (b) van Doorn, A. R.; Schaafstra, R.; Bos, M.; Harkema, S.; van Eerden, J.; Verboom, W.; Reinhoudt, D. N. *J. Org. Chem.* **1991**, *56*, 6083.

(28) Pearce, C. M.; Sanders, J. K. M. *J. Chem. Soc., Perkin Trans. 1* **1994**, 1119.

(29) Landmann, B.; Hoffmann, R. W. *Chem. Ber.* **1987**, *120*, 331.

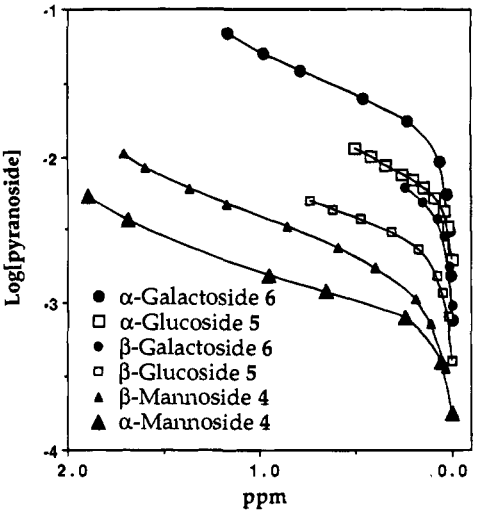

Figure 3. Average chemical shift of the four hydroxyl resonances in a pyranoside plotted from a common origin against the concentration of that pyranoside, showing the relative tendencies of pyranosides to self-associate in $CDCl_3$ at 295 K.

reinforcing the next in a cooperative manner.[24] Equatorial–axial vicinal diols in six-membered rings have stronger intramolecular hydrogen bonds than equatorial–equatorial diols[19] so the hydrogen bond from the 2-OH to the anomeric oxygen in the α anomers of glucoside **5** and galactoside **6** should be stronger than in the β anomers, and may initiate better conjugation along the rest of the hydrogen-bond chain. Likewise, the β anomer of mannoside **4** should be more hydrogen bonded than the α anomer. IR spectra of the pyranoside ligands (0.5 mM in CH_2Cl_2) showed a broad band centered at ~3585 cm^{-1} due to intramolecularly hydrogen bonded hydroxyls.[19]

(2) Intermolecular Hydrogen Bonds between Pyranosides. Assuming that aggregation is a nonspecific process governed chiefly by the ability to form intermolecular hydrogen bonds,[31] the tendency of a pyranoside to self-associate, or its self-stickiness, could be considered analogous to interaction of the sugar with an unselective receptor. The hydroxyl resonances in the ^1H NMR spectrum moved downfield in parallel and broadened as the concentration of pyranoside was increased. ^1H NMR dilution curves were obtained by plotting the average chemical shift of all the hydroxyl protons in a pyranoside against the concentration of that pyranoside (Figure 3). Variable-concentration IR spectra showed a broad band due to intermolecular hydrogen bonding at ~3400 cm^{-1} which appeared at the lowest concentrations for the most strongly aggregating sugars. Measurements of average molecular weight by vapor phase osmometry showed that α-mannoside **4** was more aggregated than β-glucoside **5** which was more aggregated than α-galactoside **6** (data given in the Experimental Section).

(3) Pyranoside–Methanol Intermolecular Hydrogen Bonds. The trend in equilibrium constants for pyranoside–methanol hydrogen bonds, considering methanol as an essentially structureless "receptor", should also reflect the balance between inter- and intramolecular hydrogen bonding. Equilibrium constants were measured by ^1H NMR titration of a dilute solution of a pyranoside in acid-free $CDCl_3$ with methanol. The four hydroxyl resonances of the pyranoside moved downfield, roughly in parallel by 1.5–2 ppm on addition of methanol (0–1.0 M), with discrete coupled resonances for all hydroxyl protons, including methanol. The average value of the equilibrium constants for the four hydroxyl resonances in a particular pyranoside was taken as a measure of the average strength of the methanol–sugar hydrogen bond for that pyranoside (K_S). The following values were obtained: β-mannoside **4**, $K_S = 1.5(\pm 0.5)$; α-mannoside **4**, $K_S \geq 2$; β-glucoside **5**, $K_S = 0.9(\pm 0.3)$; α-glucoside **5**, $K_S = 0.7(\pm 0.3)$; β-galactoside **6**, $K_S = 0.7(\pm 0.3)$; α-galactoside **6**, $K_S = 0.6(\pm 0.3)$.

The three types of evidence above define an empirical stickiness order of α-mannose > β-mannose > β-glucose > α-glucose ≈ β-galactose > α-galactose, which is essentially the same order as depicted in Figure 3. Thus, in broad terms, **Zn1** is an indiscriminate receptor since the binding order can be rationalized by the tendency of the pyranosides to form intermolecular hydrogen bonds. However several deviations from the stickiness order suggest that **Zn1** does has some inherent selectivity. A difference in binding energy of 3 kJ/mol was observed for the enantiomeric α-glucoside **5** ligands, which are necessarily intramolecularly hydrogen bonded to the same extent. The anomers of galactoside **6** are bound in the opposite order to that predicted on the basis of intramolecular hydrogen bonding. Also the lack of discrimination between the anomers of mannoside **4** may reflect some selectivity, since a much larger difference would be expected in favor of the α-anomer due to the transdiaxial arrangement of the C-1 and C-2 oxygens which disrupts formation of a cooperative ring of intramolecular hydrogen bonds. **Zn1** was not designed to bind any specific sugar derivative; the expectation was that the cavity would provide a refuge for a variety of polar substrates in organic solution. Indeed acyclic sugar amide **7** and pyranoside **8**, which is a mixture of stereoisomers, both bind strongly, and it seems likely that many other appropriately sized polyfunctional molecules would be complexed as well.

More generally, it is often tacitly assumed that for a given receptor the variation of binding energy within a series of ligands reflects interactions in the complex, whereas it may in fact reflect a variation in ground state energy of the ligands. The effect is likely to be particularly significant when recognition employs the same interactions as are responsible for altering the energy levels of the ligands, hydrogen bonding in the present case. This does not of course alter the operational consequences that in an equimolar mixture of **Zn1**, α-mannoside **4**, and β-galactoside **6**, 97% of the bound species will contain the mannose derivative, but it does imply that simpler receptors may be just as effective.

A Model for Pyranoside Binding by Zn1. A two-point binding model[13j] is first developed for pyranoside binding by the roof component of **Zn1**, dilactone **3**; once the ligand has been gripped at two points, a third interaction may then determine the details of the recognition process. It is assumed that each steroidal hydroxyl group forms one net hydrogen bond to the pyranoside. Once the first bond has formed, the second bond is now intramolecular, and the binding energy for the two-step process is $2\Delta G - RT \ln(f)$, where ΔG is the energy of the alcohol–pyranoside hydrogen bond and f is the chelation factor or effective molarity.[32] ΔG can be estimated as −4.1 kJ/mol from the equilibrium constant previously measured between methanol and β-glucoside **5**, a typical pyranoside.[33] An independent value of $-\Delta G \leq 5$ kJ/mol comes from the binding of β-glucoside **5** to diol **9**, providing an upper limit. Chelation

(30) Several arrangements of hydrogen bonds within a particular ligand are consistent with the spectroscopic results. For a detailed analysis of hydrogen bonding in partially protected pyranoside derivatives, see: Muddasani, P. R.; Bozo, E.; Bernet, B.; Vasella, A. *Helv. Chim. Acta* **1994**, *77*, 257.

(31) No correlation was found between binding energy and pyranoside solubility. Solvation energies derived from solubility measurements in any case presumably reflect the difference in energy between a molecule in a hydrogen-bonded lattice and a molecule in a hydrogen-bonded micellar aggregate. Crystalline pyranosides are known to be largely intermolecularly hydrogen bonded.[24]

(32) Kirby, A. J. *Adv. Phys. Org. Chem.* **1980**, *17*, 183.

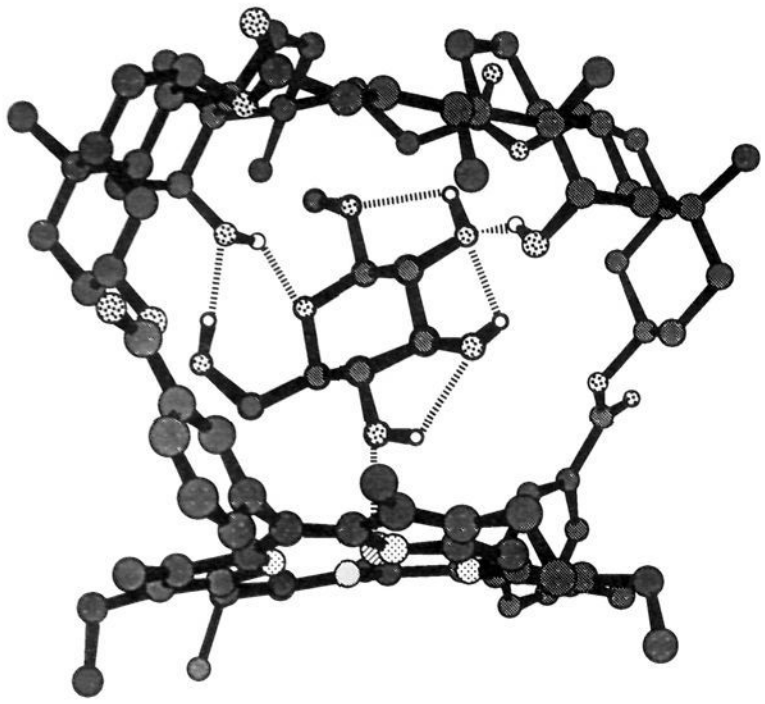

Figure 4. A possible structure for the complex formed between Zn**1** and β-glucoside **5**. The octyl solubilizing chain has been replaced by a methyl group for clarity. The Zn−O bond length (2.2 Å) and displacement of the zinc atom from the plane of the porphyrin (0.2 Å) were taken from crystal structures containing methanol or water coordinated to zinc porphyrins.[17b,c]

factors for intramolecular hydrogen bonds between hydroxyl groups range from 1 to 20 for fairly rigid systems in $CHCl_3$.[13j,10c] Thus binding energies of the order 8 to 16 kJ/mol are predicted for two-point binding of a pyranoside in the absence of any further interactions, providing a reasonable lower estimate for the data in Table 1. Due to a combination of statistical and entropic factors, two-point binding by a suitably disposed pair of hydroxyl groups can thus provide a significant driving force for pyranoside complexation in nonpolar solvents.

The capped porphyrin H_2**1** binds pyranosides better than dilactone **3** by 3−6 kJ/mol (Tables 1 and 4). This may be due to conformational differences between dilactone **3** and the cap of H_2**1** or a more vacuum-like interior. H_2**1** binds pyranosides almost as well as Zn**1** in the three cases examined (Table 4) despite the extra Lewis acid site in Zn**1**. If the floor and roof components of Zn**1** were binding pyranosides in a cooperative fashion, Zn**1** should bind e.g. β-glucoside **5** more strongly than H_2**1** by about $12 - RT \ln 4 = 8.6$ kJ/mol, where 12 kJ/mol is the binding energy of β-glucoside **5** to Zn**2**, and a statistical factor of $RT \ln 4$ has been included since only one pyranoside hydroxyl can coordinate to the zinc atom. (Here "cooperative" binding means a chelation factor $f \geq 1$.) Computer-assisted molecular modeling provided qualitative insight into the lack of difference between Zn**1** and H_2**1**, the main conclusion being that pyranosides are not bulky and three-dimensional enough to fill the cavity. Pyranosides bind mainly to the roof of H_2**1**; on incorporation of a Lewis acid site in the floor the ligand changes orientation at the expense of some favorable binding to the roof. This is in accord with different limiting chemical shifts for bound Zn**1** and H_2**1**, and hence different binding geometries.

A working hypothesis for the geometry of Zn**1** and β-glucoside **5** is shown in Figure 4. Most of the intramolecular hydrogen bonds in the ligand are retained, with a total of two new hydrogen bonds formed between ligand and receptor in addition to the zinc−oxygen bond. Weakly cooperative three-point binding accounts for enantioselective inclusion, and the statistical and entropic advantages inherent in two- or three-point binding are adequate to explain the magnitude of the binding energies observed in all solvents (see below).

(33) This is the statistical result of forming one hydrogen bond between one of the steroidal hydroxyl groups and one of up to six oxygens on the pyranoside: $-\Delta G = RT \ln(6K_S) = 4.1$ kJ/mol.

Effect of Solvent Polarity on Pyranoside Binding by Zn1. α-Mannoside **4** binds more strongly in cyclohexane than CH_2Cl_2 by 18.7 kJ/mol, more than 3 orders of magnitude in equilibrium constant (Table 5). The structures of the complexes formed in CCl_4 and cyclohexane appear to be similar to those in CH_2Cl_2 since the UV λ_{max} shifts for free and bound Zn**1** in these solvents parallel those of uncapped porphyrin Zn**2**, suggesting no solvent-induced change in binding geometry. Also the low-temperature, slow-exchange ^{1}H NMR spectra of β-glucoside **5** bound to Zn**1** in CH_2Cl_2 and CCl_4 are similar, implying that the structure of the complex is also similar in these two solvents.

The increased binding of α-mannoside **4** by 13.4 kJ/mol in CCl_4 and 18.7 kJ/mol in cyclohexane relative to CH_2Cl_2 can be rationalized on the basis of the relative strengths of alcohol−alcohol and alcohol−zinc bonds in these solvents, in addition to smaller contributions due to cavity solvation.[34] The difference in binding energy between CH_2Cl_2 and another solvent is given by $\Delta\Delta G = \Delta\Delta G_{hbond} + \Delta\Delta G_{Zn-O} + \Delta\Delta G_{solv} - \Delta[RT \ln (f)]$ where $\Delta\Delta G_{hbond}$ and $\Delta\Delta G_{Zn-O}$ are the differences in hydrogen bond and zinc−oxygen bond strengths in the two solvents, $\Delta\Delta G_{solv}$ represents differential solvation of the cavity and ligand, and $\Delta[RT \ln (f)]$ is the difference in chelation factor in the two solvents. The following assumptions are now made:

(1) The $\Delta\Delta G_{hbond}$ term can be estimated from the relative strength of the methanol−methanol hydrogen bond in the two solvents, experimentally $-\Delta\Delta G_{hbond} = 6.2$ kJ/mol in CCl_4 and $-\Delta\Delta G_{hbond} = 8.2$ kJ/mol in cyclohexane.[23a]

(2) The $\Delta\Delta G_{Zn-O}$ term can be estimated from the relative strength of the methanol−Zn**2** interaction in the two solvents, experimentally $-\Delta\Delta G_{Zn-O} = 3.1$ kJ/mol in CCl_4, and $-\Delta\Delta G_{Zn-O} \geq 4.8$ kJ/mol in cyclohexane.

(3) Introduction of a small molecule such as pyrazole **12** into the cavity disrupts solvation to the same extent as a pyranoside. Relative to CH_2Cl_2, pyrazole binding to Zn**1** was enhanced in CCl_4 by $-\Delta\Delta G_{solv} = 1.7$ kJ/mol and in cyclohexane by 3.7 kJ/mol.[35]

(4) Chelation factors are, to a first approximation, independent of solvent i.e. $\Delta[RT \ln (f)] = 0$.

Adding together the terms, the predicted binding increases relative to CH_2Cl_2 are 11 kJ/mol in CCl_4 and 16.7 kJ/mol in cyclohexane, of the same order as the experimental values. This type of analysis provides a physically reasonable explanation for the large solvent effects. The binding energy of α-mannoside **4** to Zn**1** in cyclohexane, one of the largest reported for a hydrogen-bonding receptor ($K = 3 \times 10^7$ in dry solvent at 295 K, rising to $> 10^8$ if methanol is added), is thus essentially an example of solvophobic forcing.

Effect of Added Water and Methanol on Pyranoside Binding by Zn1. Stronger binding was seen if small amounts of methanol or water were added to solvents used for UV or NMR titrations (Table 5). Addition of bulky alcohols such as isopropyl alcohol and *tert*-butyl alcohol resulted in weaker binding. UV titrations of Zn**1** in the presence of water or methanol were essentially isosbestic implying that all species

(34) For simplicity pyranoside binding to Zn**1** is viewed, from a thermodynamic point of view, as a moderately cooperative two-point interaction with one zinc−oxygen bond and one hydrogen bond, rather than the weakly cooperative three-point interaction pictured in Figure 4.

(35) $\Delta\Delta G_{solv}$ is defined as the difference in binding energy between Zn**1** and Zn**2** in CCl_4 or cyclohexane minus the difference in CH_2Cl_2, thus factoring out variation in the zinc−nitrogen bond energy. Pyrazole-derived energies may underestimate pyranoside solvation energies; pyranosides bind to H_2**1** better in $CHCl_3$ than in CH_2Cl_2 by on average 3.7 kJ/mol (Table 4), whereas increased binding of only $-\Delta\Delta G_{solv} = 0.6$ kJ/mol would be predicted.

Table 5. Dependence of Binding Energies (kJ/mol) of Pyranosides to Zn**1** on Solvent Polarity and Added Water on Methanol

		$-\Delta G^a$		
pyranoside	solvent	dry	$+H_2O$	+MeOH
β-D-glucoside (**5**)	$CHCl_3$	19.6	24.3(0.050)[b]	
β-D-glucoside (**5**)	CH_2Cl_2	17.9	21.6(0.090)	19.4(0.125)[b]
β-D-mannoside (**4**)	CH_2Cl_2	21.0	24.1(0.095)	22.7(0.125)
α-D-mannoside (**4**)	CH_2Cl_2	21.7	23.1(0.090)	24.2(0.125)
α-D-mannoside (**4**)	CCl_4	35.1	36.6(0.006)	39.0(0.012)
α-D-mannoside (**4**)	cyclohexane	40.4		>45.0(0.004)[c]

[a] $\Delta G = RT \ln(K)$. K determined by UV and/or ^1H NMR titration at 295 K. [b] Concentration of added water or methanol (mol/L) in titration solvent. [c] K to large to measure accurately.

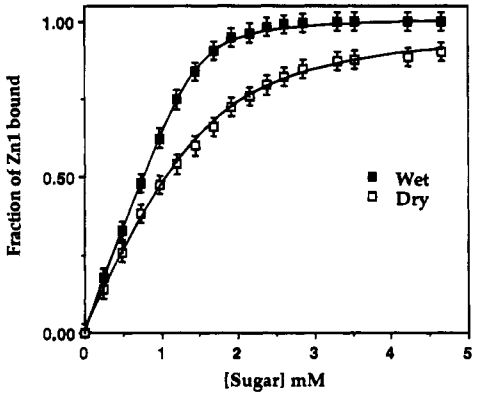

Figure 5. ^1H NMR titration of Zn**1** (1.5 mM) with β-glucoside **5** in wet and dry $CDCl_3$ showing stronger binding in wet solvent. The average chemical shift for the four most sensitive receptor resonances is plotted for both curves, error bars corresponding to ±1 Hz. Wet $CDCl_3$ was 47 mM in water by integration. Completely anhydrous solvent was obtained by adding a very small quantity (<0.1 mg) of 4 Å sieves to the NMR tube.

have similar extinction coefficients. The experimental results were well fitted by a simple 1:1 binding model, resulting in an overall or observed binding energy $\Delta G_{obs} = -RT \ln K_{obs}$. Experimental results for ^1H NMR titration of Zn**1** with β-glucoside **5** in dry and wet $CDCl_3$ are shown in Figure 5. Analyzed as a simple 1:1 complexation, the equilibrium constant increased from $K_{obs} = 3(\pm1) \times 10^3$ in dry $CDCl_3$ to $K_{obs} = 2(\pm1) \times 10^4$ in $CDCl_3$ containing 47 mM water. Some of the chemical shifts of the bound receptor were significantly different in wet solvent, showing that a different species had been formed.

Methanol was used to investigate synergistic binding in detail because it is completely miscible in most organic solvents. As the concentration of methanol in the titration solvent was increased the observed binding energy first increased, reaching a maximum at about 0.5% v/v methanol (in CH_2Cl_2), and then decreased to below its value in dry solvent as shown in Figure 6. According to a simple model (Figure 7) ΔG_{obs} is the resultant of three competing processes:

(1) Added polar species solvate the sugar (K_S), shifting the overall equilibrium to the left and decreasing the observed equilibrium constant, $K_{obs} < K_1$, where K_1 is the equilibrium constant in pure solvent.

(2) Added polar species solvate the receptor (K_3, K_4, ..., K_N), reducing the observed equilibrium constant, $K_{obs} < K_1$.

(3) Added polar species solvate the sugar–receptor complex (K_2) shifting the overall equilibrium to the right, increasing the observed equilibrium constant, $K_{obs} > K_1$.

In order to check the basic features of the model a quantitative treatment of observed binding energy as a function of methanol is presented below. If the simplifying assumption is made that all species have identical extinction coefficients, then the binding

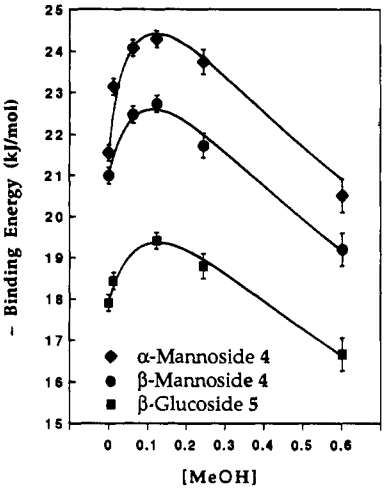

Figure 6. Effect of varying the concentration of added methanol (mol/L) on the binding energy of pyranosides to Zn**1** in CH_2Cl_2, with best fit curves used to obtain K_2 values.

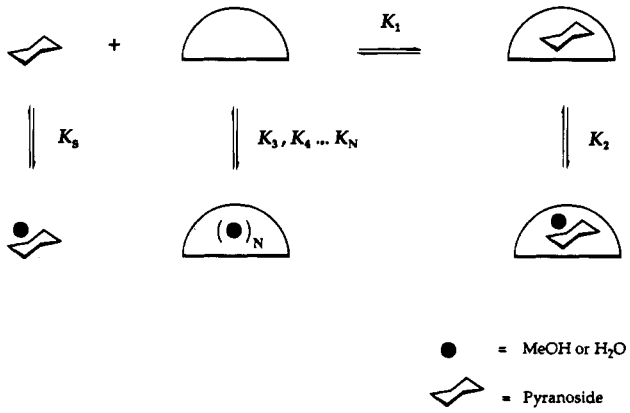

Figure 7. Analysis of binding enhancement of pyranosides in wet or methanolic solvents in terms of solvation of ligand (K_S), receptor (K_3, ..., K_N) and complex (K_2).

curve has the same functional form as a simple 1:1 binding curve (see data analysis section of the experimental), with the consequence that the best fit equilibrium constant K_{obs} can be expressed simply as a combination of the various equilibria in Figure 7:

$$K_{obs} = K_1 \frac{\{1 + K_2 L_2\}}{\{1 + \alpha\}\{1 + \beta\}} \quad (1)$$

where K_1 is the equilibrium constant in dry solvent, L_2 is the concentration of added water or methanol, $\alpha = K_S L_2$ represents sugar solvation, and $\beta = K_3 L_2(1 + K_4 L_2(1 + K_5 L_2))$ represents receptor solvation. Since the binding of methanol to Zn**1** and pyranosides has already been quantified, eq 1 allowed calculation of the complex solvation term, K_2.[36]

Best-fit curves treating K_2 as a variable parameter and using experimental values for K_1, K_3, K_4, and K_5 are shown in Figure 6. The binding enhancements $-\Delta G_2 = RT \ln K_2$ due to incorporation of methanol into the receptor–sugar complex in CH_2Cl_2 were thus found to be 9.5 kJ/mol for α-mannoside **4**, 7.5 kJ/mol for β-mannoside **4**, and 7.0 kJ/mol for β-glucoside **5**. A similar curve was obtained for α-mannoside **4** in CCl_4, yielding a binding enhancement of $-\Delta G_2 = 15$ kJ/mol, the main difference being that the maximum binding occurred at much lower concentrations of methanol.[37]

(36) It is assumed that the K_S values measured in $CDCl_3$ are likely to be similar in CH_2Cl_2.

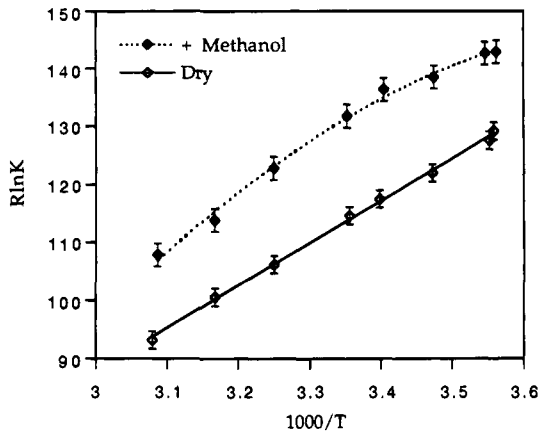

Figure 8. Van't Hoff plot for Zn1 plus α-mannoside **4** in dry CCl_4 (solid line) and with the addition of 0.05% v/v methanol (dotted curve).

These ΔG_2 values represent the maximum extra binding energy possible in the absence of receptor and ligand solvation. The experimentally observed binding enhancements (at a particular concentration of methanol) are lower due to varying degrees of competition by methanol for the binding site and sugar ligand. A single molecule of methanol is assumed to participate in complex solvation; simulation implied that while the involvement of more than one molecule cannot be ruled out, additional binding steps are probably weak. The quality of the (one parameter) fits between predicted binding energies and experimental data in Figure 6 suggests that a reasonably complete description of solvation at the molecular level has been achieved.

Effect of Methanol on Thermodynamics of α-Mannoside 4 Binding by Zn1. The results of variable-temperature UV titration in dry CCl_4 and in 0.05% v/v methanolic CCl_4 are shown in Figure 8. In dry solvent the van't Hoff plot was linear within experimental error, giving $\Delta H = -73(\pm 5)$ kJ/mol and $-T\Delta S = +38$ kJ/mol at 295 K. In methanolic CCl_4, plotting $R \ln K_{obs}$ against $1/T$ resulted in a curve. Bent van't Hoff plots are generally interpreted as evidence that initial and final states have different heat capacities (ΔC_p),[38,39] although the origin of the effect is often uncertain. Here it is qualitatively clear how a negative heat capacity can arise, although experimental limitations precluded a complete analysis in terms of the temperature dependence of equation 1.[40] As the temperature is lowered the binding site becomes increasingly saturated with methanol due to the cooperative nature of the binding process, rapidly outcompeting the sugar ligand, and reducing the apparent enthalpy (downward curvature in Figure 8). This is equivalent to adding more methanol at room temperature, which leads to a reduction in binding energy (downward curvature in Figure 6). A ΔC_p of this sort is only expected if equilibrium constants are measured over a temperature range in which there are appreciable concentrations of partially solvated species.

At room temperature, the enthalpies in methanolic and dry solvent are roughly the same, since the tangent to the van't Hoff plot in methanolic solvent is approximately parallel to that in dry solvent. Hence the order of magnitude increase in equilibrium constant in methanolic solvent (K increasing from $\sim 10^6$ to $\sim 10^7$) arises from entropically favorable release of polar cosolvent. A net favorable entropic component due to solvent release implies that solvation of ligand and receptor by methanol, which is expected to be an enthalpically weak process, is associated with a relatively greater unfavorable entropic penalty than specific solvation of the receptor–ligand complex, which is expected to be an enthalpically stronger interaction.[41]

Despite recent experimental[42a,b] and computational[42c] advances, there is little quantitative information available on functional group solvation in either water or organic solvents. If CCl_4 is considered as a gaslike essentially inert solvent, then exploration of hydrogen-bonding systems in which solvation, considered as a series of equilibria, can be *quantified* offers an interesting opportunity to explore solvent effects in recognition at a molecular level. Wet or alcoholic nonpolar solvents can be thought of as "dilute water", in effect a model for the first steps of aqueous hydration but without the complications of having to explicitly consider effects due to the bulk hydrogen-bonded structure of water. Quantitative studies of this sort might be expected to further the understanding of hydrogen bonding receptors designed to operate in more competitive solvents.[43]

Synergistic Binding of Misfit Guests. Addition of a polar cosolvent to a well-matched receptor–ligand pair in nonpolar solution would normally be expected to reduce binding, since solvation of exposed polar functional groups in the reactants is likely to be better (more negative ΔG) than solvation of "satisfied" functional groups in the adduct, i.e. the free energy of the reactants will be lowered more than the product. Indeed Adrian and Wilcox[44] reported that association in wet $CHCl_3$ was weaker than in dry $CHCl_3$ for a hydrogen-bonding receptor, and showed that this was because the unfavorable enthalpic terms due to receptor and ligand solvation outweighed positive entropic terms due to solvent release on complexation.

The unprecedented binding *increase* in wet or methanolic solvents found for Zn1 and sugar ligands demonstrates that solvation of the product complex in a poorly matched receptor pair can be better than solvation of the reagents, i.e. the free energy of the product is lowered more than the reactants. It was concluded above on the basis of binding energies and modeling studies that pyranoside ligands are misfit guests which do not geometrically exploit the full recognition potential of the host cavity, leaving "unsatisfied" functional groups. This gives water or small polar species the opportunity to fill in the gaps between receptor and ligand, presumably strengthening or extending the intermolecular hydrogen-bond network (equally valid descriptions of this effect are that a partially solvated ligand fits the receptor better or that a partially solvated receptor is

(37) Ligand solvation could not be measured directly, since α-mannoside **4** is largely aggregated at NMR concentrations in CCl_4. Assuming that ligand solvation is likely to be better in CCl_4 than in CH_2Cl_2 by the same factor that the equilibrium constant for the methanol–methanol hydrogen bond is larger, K_S for α-mannoside **4** in CCl_4 was estimated as ~25, and simulation of binding energy as a function of methanol concentration gave a good fit.

(38) Diederich, F.; Smithrud, D. B.; Sanford, E. M.; Wyman, T. B.; Ferguson, S. B.; Carcanague, D. R.; Chao, I.; Houk, K. N. *Acta Chim. Scand.* **1992**, *46*, 205.

(39) Stauffer, D. A.; Barrans, R. E., Jr.; Dougherty, D. A. *J. Org. Chem.* **1990**, *55*, 2762.

(40) This was mainly due to the difficulty in obtaining accurate enthalpies for the weak solvation processes. Systematic errors inherent in extracting three equilibrium constants from a methanol–Zn1 binding isotherm (two of which are shown in Figure 2) resulted in unacceptably large errors during subsequent van't Hoff treatment.

(41) The variation in the extent of enthalpy/entropy compensation with magnitude of the enthalpy has been advanced as the physical basis of "entropy-driven" binding in organic solution: Searle, M. S.; Westwell, M. S.; Williams, D. H. *J. Chem. Soc., Perkin Trans. 2*, in press.

(42) (a) Tsai, R.-S.; Fan, W.; El Tayer, N.; Carrupt, P.-A.; Testa, B.; Kier, L. B. *J. Am. Chem. Soc.* **1993**, *113*, 9632 and references therein. (b) Christian, S. D.; Taha, A. A.; Gasg, B. W. *Q. Rev. Chem. Soc.* **1970**, *24*, 20. (c) Jorgensen, W. L. *Acc. Chem. Res.* **1989**, *22*, 184.

(43) (a) Fan, E.; Van Armen, S. A.; Kincaid, S.; Hamilton, A. D. *J. Am. Chem. Soc.* **1993**, *115*, 369. (b) Rotello, V. M.; Viani, E. A.; Deslongchamps, G.; Murray, B. A.; Rebek, J., Jr. *J. Am. Chem. Soc.* **1993**, *115*, 797.

(44) (a) Adrian, J. C., Jr.; Wilcox, C. S. *J. Am. Chem. Soc.* **1992**, *114*, 1398. (b) Adrian, J. C., Jr.; Wilcox, C. S. *J. Am. Chem. Soc.* **1991**, *113*, 678.

more complementary to the ligand). This type of intercalation is well known for biological recognition processes,[45] but does not appear to have been reported for organic-soluble synthetic systems.[46]

Water molecules would be expected to be particularly good at gluing together polar but noncomplementary molecules due their hydrogen-bonding ability and small size. Since there is a limited amount of space under the cap when a pyranoside has bound it is understandable that while methanol is small enough to fit between ligand and receptor, bulky alcohols isopropyl alcohol and *tert*-butyl alcohol show no synergistic binding enhancements. The ΔG_2 values for intrinsic binding enhancement by methanol show that the recognition ability of **Zn1** can be not only enhanced, but also *modulated* by the addition of polar cosolvents, albeit over a limited range.

Comparison with Natural Receptors.[47-49] Recognition in water may be considered as a stepwise process involving (1) desolvation of receptor and ligand, (2) gas-phase binding, and (3) resolvation of the complex. While pyranoside recognition in nonpolar organic solution most closely resembles the gas-phase step, addition of a polar cosolvent begins to include features of steps 1 and 3, and some comparisons between natural receptors and **Zn1** are worth making. It has been suggested that conclusions about sugar binding sites based on the binding energies of different ligands may be affected by differing degrees of aqueous solvation of the ligand.[47d] It was shown above that synergistic binding enhancement depends on the degree of ligand solvation by methanol, and also that selectivities in dry solvent could be rationalized by differing degrees of internal solvation within the ligand. Several sugar-binding proteins have hydrophobic regions in the binding site, and it has been suggested that parts of the bound sugar in these regions could be made more hydrophobic by intramolecular hydrogen bonding.[47c] which would also recoup some of the energy lost on desolvation of the hydroxyl groups. Pyranoside derivatives were shown to be largely intramolecularly hydrogen-bonded in nonpolar solution, mimicking a hydrophobic receptor environment. Sugar–sugar interactions are thought to be important in cellular recognition.[47e] The self-association of pyranosides derivatives could be considered as a simple model for this process. Of most direct relevance are reports by Quiocho et al.[48] and Boume et al.[49] on the unusually important role of water in sugar recognition by a group of proteins which have high affinities for simple monosaccharides. Crystal structures of the protein–sugar complexes revealed one or more water molecules firmly embedded in the protein–sugar hydrogen bond network, both mediating and modulating monosaccharide recognition. There is a striking parallel here with the role postulated for added water or methanol in enhancing and modulating sugar binding to **Zn1** by bridging between receptor and ligand functional groups.[45,50]

Summary and Concluding Remarks

Hemispherical dilactone **3** was introduced as a novel cleftlike receptor for pyranosides, and a simple two-point binding model proposed. Lewis acid-induced polarization of alcohols bound to **Zn2** and **ZnTPP** was found to promote further inter- and intramolecular hydrogen bonding. The combination of dilactone **3** and **Zn2** as roof and floor components of **Zn1** produced a receptor with the chirality and recognition properties of **3** and the metal site and spectroscopic advantages of the porphyrin chromophore. The free base porphyrin H_2**1** bound pyranosides almost as effectively as **Zn1**, but in different orientations. This may be a useful feature of H_2**1**, since if strong binding is possible without the Lewis acid site, then the superstructure may be able to position ligands over more chemically versatile metalloporphyrins.

The binding selectivity of **Zn1** was related to both the inherent receptor selectivity and the degree of intramolecular hydrogen bonding in the ligand. The "stickiness" order proposed for organic soluble pyranosides applies to any hydrogen bonding receptor for this type of ligand.[8,9c,e,13a,g] The large solvent effects observed for pyranoside inclusion were semiquantitated on the basis of the strengths of hydrogen bond and the zinc–oxygen interactions in different solvents, with smaller contributions due to cavity and ligand desolvation.

Based on the idea of ligand–receptor mismatch, and the ability of **Zn1** to bind several species it was demonstrated that pyranoside binding could be both enhanced and modulated by addition of small hydrogen-bonding species. Water was shown to be incorporated into the ligand–receptor complex by ^{1}H NMR, and methanol-induced binding enhancement successfully modeled on the basis of a series of solvation equilibria. It was concluded that, in a process characterized by a negative heat capacity, the enthalpic advantage of methanol incorporation outweighed the entropic disadvantage of termolecular complex formation, resulting in overall entropy-driven binding due to solvent release. This gap-filling approach may represent a general strategy for sequestering misfit guests. Finally several parallels were drawn between hydrogen-bonded recognition of sugars in nonpolar media and natural receptors operating in aqueous solution, most notably the involvement of water in the recognition process.

Experimental Section

General. NMR spectra were recorded on Bruker WM-250 or AM-400 spectrometers. Chemical shifts in $CDCl_3$ are given relative to $CHCl_3$ (7.25 ppm J values in hertz). UV–visible spectra were recorded on a Perkin-Elmer Lambda 2 instrument with a thermostated cell holder. IR spectra of polyols were recorded on a Perkin-Elmer 1600 series FTIR spectrophotometer in 1 mm or 10 mm cells in dry CH_2Cl_2. The residual water peak at ~3700 cm^{-1} was removed by adding one or two 4 Å sieve beads to the cell. Equilibrium constants for intramolecular hydrogen bonding of α,ω-diols were calculated as detailed in ref 21. Apparent solution molecular weights were determined in dry ethanol-free chloroform using a Wescor 5500 vapor-phase osmometer operating at 37 °C. An accurate calibration curve was constructed over the range of instrument response observed for alkyl pyranosides using standard solutions of glucoside pentaacetate (Sigma) and benzil (recrystallized). For β-glucoside **5** at 37 °C in $CHCl_3$ the following

(45) *Water and Biological Macromolecules*; Westhof, E., Ed.; Macmillan Press: New York, 1993.

(46) For the synergistic binding of cosolvents to cyclodextrins in water see, for example: (a) Tee, O. S.; Bozzi, M. *J. Am. Chem. Soc.* **1990**, *112*, 7815. (b) Ueno, A.; Moriwaki, F.; Osa, T.; Ikeda, T.; Toda, F.; Hattori, K. *Bull. Chem. Soc. Jpn.* **1986**, *59*, 3109. For a study of hydration in organic crystals, see: (c) Desiraju, G. R. *J. Chem. Soc., Chem. Commun.* **1991**, 426.

(47) (a) Sharon, N.; Lis, H. *Chem. Br.* **1990**, 679. (b) Lemieux, R. U. *Chem. Soc. Rev.* **1989**, *18*, 347. (c) Lemieux, R. U.; Boullanger, P. H.; Bundle, D. R.; Baker, D. A.; Nagpurkar, A.; Venot, A. *New J. Chem.* **1978**, *2*, 321. (d) Carver, J. P. *Pure Appl. Chem.* **1993**, *65*, 763. (e) Hokamori, S. *Pure Appl. Chem.* **1991**, *63*, 473.

(48) (a) Quiocho, F. A. *Pure Appl. Chem.* **1989**, *61*, 1293. (b) Quiocho, F. A.; Wilson, D. K.; Vyas, N. K. *Nature* **1989**, *340*, 404. (c) Vyas, N. K.; Vyas, M. N.; Quiocho, F. A. *Science* **1988**, *242*, 1290.

(49) (a) Bourne, Y.; Roussel, A.; Frey, M.; Rougé, P.; Fontecilla-Camps, J. C.; Cambillau, C. *Proteins* **1980**, *8*, 365. (b) Bourne, Y.; Rougé, P.; Cambillau, C. *J. Biol. Chem.* **1990**, *265*, 18161.

(50) The importance of water-mediated recognition in aqueous solution is becoming increasing apparent from high-resolution crystal structures. For a recent example of enthalpically driven multiple packing of waters between an antibody and its antigen, see: Bhat, T. N.; Bentley, G. A.; Boulot, G.; Greene, M. I.; Tello, D.; Dall'Acqua, W.; Souchon, H.; Schwartz, F. P.; Mariuzza, R. A.; Poljak, R. J. *Proc. Natl. Acad. Sci. U.S.A.* **1994**, *91*, 1089.

degrees of aggregation were obtained, expressed as the average number of monomer units: 1.75mer at 10 mM, 3.5mer at 15 mM, 6.1mer at 30 mM, and 16.5mer at 110 mM.[51] At 10 mM α-mannoside **4** was a 3.2mer and α-galactoside **6** a 1.2mer. Computer assisted molecular modeling employed MacroModel (3.0)[52] using Amber or MM2 force fields.

Ligands. Commercially available amine, alcohol, and diol ligands were recrystallized or distilled before use to remove traces of acid and water. Pyranoside ligands were purified by chromatography (10% MeOH in CH_2Cl_2) unless otherwise indicated. Below are listed ^{1}H NMR assignments for monomeric, or largely monomeric, pyranosides in $CDCl_3$ (1.7 to 5 ppm, the assignment of pairs of resonances marked with an asterisk (*) may be reversed) along with characterization data for new compounds. ***n*-Octyl β-D-glucopyranoside 5** (Sigma, used as received): ^{1}H NMR (1.0 mM in $CDCl_3$) 1.96 (t, J = 6.5, 1H, 6-OH), 2.37 (d, J = 2.1, 1H, 2-OH), 2.48 (d, J = 2.4, 1H, 3-OH*), 2.61 (d, J = 1.8, 1H, 4-OH*), 3.35 (td, 1H, 2-H), 3.40 (m, 1H, 5-H), 3.52 (m, 1H, OCH_2CH$_2$), 3.57 (td, 1H, 4-H*), 3.61(td, 1H, 3-H*), 3.83 (m, 1H, 6-H), 3.89 (m, 1H, OCH_2CH$_2$), 3.91 (m, 1H, 6-H), 4.30 (d, J = 7.9, 1H, 1-H). ***n*-Octyl α-D-glucopyranoside 5** (Sigma, used as received) and ***n*-octyl α-L-glucopyranoside 5**:[9c] ^{1}H NMR (2.0 mM in $CDCl_3$) 1.91 (dd, J = 5.8, 7.0, 1H, 6-OH), 1.99 (d, J = 10.8, 1H, 2-OH), 2.48 (d, J = 2.8, 1H, 3-OH*), 2.57 (d, J = 2.4, 1H, 4-OH*), 3.43 (m, 1H, OCH_2CH$_2$), 3.46 (td, 1H, 2-H), 3.56 (td, 1H, 4-H*), 3.72 (td, 1H, 3-H*), 3.67 (m, 1H, 5-H), 3.73 (m, 1H, OCH_2CH$_2$), 3.8–3.9 (m, 2H, 2 × 6-H), 4.85 (d, J = 3.6, 1H, 1-H). ***n*-Decyl β-D-galactopyranoside 6**,[53] fine crystals from chloroform, mp 95 °C; when crystalline, this compound proved to be rather insoluble in CH_2Cl_2: ^{1}H NMR (1.5 mM in $CDCl_3$) 2.07 (dd, J = 5, 7.5, 1H, 6-OH), 2.36 (d, J = 1.8, 1H, 2-OH), 2.59 (d, J = 4.3, 1H, 3-OH), 2.77 (d, J = 3.0, 1H, 4-OH), 3.51 (m, 1H, OCH_2CH$_2$), 3.55 (m, 1H, 5-H), 3.60 (dd, 1H, 3-H), 3.65 (dt, 1H, 2-H), 3.89 (m, 1H, 6-H), 3.91 (m, 1H, OCH_2CH$_2$), 3.99 (m, 1H, 6-H), 4.02 (brq, 1H, 4-H), 4.26 (d, J = 7.3, 1H, 1-H); ^{13}C (100 MHz, DMSO) 103.56 (1-C), 75.20, 73.60, 70.65, 68.56, 68.23, 60.50. ***n*-Decyl α-D-galactopyranoside 6** was obtained from galactose and decanol using a modified Fischer glycosidation procedure[54] in 10% yield as an amorphous solid, mp 54–56 °C: ^{1}H NMR (7 mM in $CDCl_3$) 1.94 (d, J = 10.5, 1H, 2-OH), 2.27 (dd, J = 4.4, 7.5, 1H, 6-OH), 2.62 (d, J = 3.8, 1H, 3-OH), 2.89 (brs, 1H, 4-OH), 3.45 (m, 1H, OCH_2CH$_2$), 3.72 (m, 1H, OCH_2CH$_2$), 3.77 (dd, 1H, 3-H), 3.80 (dd, 1H, 2-H), 3.85 (m, 1H, 6-H), 3.95 (m, 1H, 6-H), 4.09 (brq, J = 3.2, 1H, 4-H), 4.95 (d, J = 3.8, 1H, 1-H); ^{13}C (100 MHz, DMSO) 98.96 (1-C), 71.21, 69.73, 68.95, 68.52, 67.02, 60.68. Anal. Calcd for $C_{16}H_{32}O_6$: C, 59.97; H, 10.07. Found: C, 60.02; H, 10.01. ***n*-Decyl α-D-mannopyranoside 4**[54,55] was obtained from galactose and decanol using a modified Fischer glycosidation procedure[54] in 40% yield as a slowly crystallizing waxy solid, mp 64–65 °C. The hydroxyl resonances of this strongly aggregating ligand could not be reliably assigned: ^{1}H NMR (0.4 mM in $CDCl_3$) 2.05, 2.3, 2.4, 2.45 (4 × brs, 4 × OH), 3.5–4.0 (m, 9H), 4.86 (d, J = 1.6, 1H, 1-H); ^{13}C (100 MHz, DMSO) 99.83 (1-C), 74.01, 71.14, 70.51, 67.09, 66.29, 61.37. ***n*-Decyl β-D-mannopyranoside 4** was obtained by the literature procedure for a similar compound[56] and crystallized as fine needles from CH_2Cl_2, mp 91 °C: ^{1}H NMR (0.8 mM in $CDCl_3$) 2.04 (t, J = 6.7, 1H, 6-OH), 2.36 (d, J = 2.1, 1H, 2-OH), 2.41 (d, J = 2.4, 1H, 4-OH), 2.48 (d, J = 9.8, 1H, 3-OH), 3.30 (m, 1H, 5-H), 3.50 (m, 1H, 3-H), 3.53 (m, 1H, OCH_2CH$_2$), 3.75 (td, J = 9.5, 2.4, 4-H), 3.83 (m, 1H, 6-H), 3.90 (m, 1H, OCH_2CH$_2$), 3.92 (m, 1H, 6-H), 4.00 (m, 1H, 2-H), 4.53 (d, J = 1, 1H, 1-H); ^{13}C (100 MHz, DMSO) 100.36 (1-C), 77.61, 73.84, 70.69, 68.48, 67.30, 61.50. Anal. Calcd for $C_{16}H_{32}O_6$: C, 59.97; H, 10.07. Found: C, 59.78; H, 10.12.

UV–Visible Titrations. A solution of ligand was added in portions via microsyringe to a solution of porphyrin host (ca. 2 μM, initial absorbance ca. 1) in a thermostated cuvette. Absorbance readings were taken at four or six wavelengths covering the Soret bands of both host and complex, with volume changes due to ligand addition being taken into account during analysis. For routine 1:1 titrations 10 to 15 ligand additions were made, covering 0–95% of the binding isotherm, ligand solubility and equilibrium constant permitting. For isobestic point checks at constant porphyrin concentration, the ligand solution was made up with the same stock porphyrin solution as in the cuvette. For multiple binding, titrations were generally done at constant porphyrin concentration with 15 to 25 ligand additions. Van't Hoff plots were derived from full titrations in the temperature range 5 to 55 °C. For titrations of **Zn1** with pyranosides in dry CCl_4 or cyclohexane, which are sensitive to small quantities of water in the solvent, one or two 4 Å sieve beads were added to the cuvette. CH_2Cl_2 for UV titrations was freshly distilled from CaH_2. CCl_4 was distilled from $CaCl_2$ and stored over molecular sieves. Reagent grade $CHCl_3$ was washed several times with water to remove ethanol, dried ($MgSO_4$), eluted through a column of activated neutral alumina (FLUKA) collecting the middle portion of the eluate under argon, and used immediately. Cyclohexane was distilled from CaH_2 and stored over 4 Å molecular sieves. Completely pure CCl_4 and $CHCl_3$ are noticeably unstable, generating significant amounts of acid if exposed to light, so titrations with these solvents were conducted as rapidly as possible, while still allowing sufficient time to attain thermal and chemical equilibrium (1 to 3 min) after each ligand addition.

^{1}H NMR Titrations. A solution of ligand was added in portions via microsyringe to a solution of host in a septum-capped NMR tube. Volume changes were taken into account during analysis. Job plots were obtained by adding sufficient solvent along with ligand solution to keep the total concentration of receptor and ligand constant. In CCl_4 or when concentrated solutions of alcohols in $CDCl_3$ were being examined, a MeOH-d_4 capillary was used as external reference. $CDCl_3$ was stored over anhydrous K_2CO_3 which serves to deacidify and partially dry the solvent (ca. 3 mM residual water). To obtain completely anhydrous $CDCl_3$ a *very* small quantity of powdered 4 Å sieves (ca. 0.1 mg) was added to the NMR tube, just enough to completely remove the water peak at 1.54 ppm, prior to ligand addition. Provided a sufficiently small quantity of sieves is used, adsorption of polar species other than water is minimal as determined by integration with respect to an internal reference, and shimming is not noticeably affected. If deacidified $CDCl_3$ is used and NMR tubes and syringes are clean and dry, no other precautions are necessary to routinely observe coupled hydroxyl protons.[28] It is important that CHOH coupling be visibly maintained during titrations since this provides an upper limit on the rate of intermolecular proton transfer and hence the extent of signal averaging, a potential source of error if peak positions are being analyzed. The 12-O*H* doublet of dilactone **3**, which is normally hidden under other steroidal resonances, was located during titrations by decoupling difference on the 12β proton. While uncatalyzed intermolecular proton exchange is slow enough on the chemical shift timescale to observe couplings of ≥1 Hz,[57] it is generally fast enough on the relaxation timescale (at *RT*) to allow saturation transfer.[58] In practice irradiation of any hydroxyl resonance in the spectrum of a polyol provides a convenient way of locating all the other hydroxyl resonances by difference spectroscopy during titrations.

Data Analysis. The equation used for analyzing UV titration data for equilibrium constants less than ~1 × 10^4 (weak binding approximation) was of the general form:

$$A_{exp} = A_i + (A_f - A_i)F$$

where A_{exp} is the experimental abosrbance, A_i is the initial absorbance, A_f is the final, fully bound absorbance, and F is a function of equilibrium constants and ligand concentrations, depending on stoichiometry. For 1:1 binding $F = K_1L_o/(1 + K_1L_o)$ where K_1 is the equilibrium constant and L_o is the total concentration of added ligand. For 1:2 stoichiometry (receptor/ligand) $F = K_1L_o(1 + K_2L_o)/(1 + K_1L_o(1 + K_2L_o))$ where K_2

(51) These values are slightly higher than those reported in ref 13g.

(52) Mohamadi, F.; Richards, N. G. J.; Guida, W. C.; Liskamp, R.; Lipton, M.; Caulfield, C.; Chang, G.; Hendrickson, T.; Still, W. C. *J. Comput. Chem.* **1990**, *11*, 440.

(53) Vill, V.; Böcker, T.; Thiem, J.; Fischer, F. *Liquid Crystals* **1989**, *6*, 349.

(54) Konradsson, P.; Roberts, C.; Fraser-Reid, B. *Recl. Trav. Chim. Pays-Bas* **1991**, *110*, 23.

(55) Brown, G. M.; Dubreuil, P.; Ichhaporia, F. M.; Desnoyers, J. E. *Can. J. Chem.* **1970**, *48*, 2525.

(56) Kaur, K. J.; Hindsgaul, O. *Glycoconjugate J.* **1991**, *8*, 90.

(57) Grunwald, E.; Jumper, C. F.; Meiboom, S. *J. Am. Chem. Soc.* **1962**, *84*, 4664.

(58) Sanders, J. K. M.; Hunter, B. K. *Modern NMR Spectroscopy*, 2nd ed.; Oxford University Press: Oxford, 1993.

is the equilibrium constant for second binding and both bound species are assumed to have identical extinction coefficients. Aggregation of methanol was assumed to be of minor importance in CH_2Cl_2 over the concentration range used for methanol titrations (0−1 M). ^{1}H NMR dilution studies of methanol in $CDCl_3$ gave an approximate value for the equilibrium constant of MeOH dimerization of $K \approx 0.2(\pm 0.1)$ using a variety of models[23d] with two variable parameters (K and a limiting chemical shift). Triple solvation of **Zn1** by methanol in CCl_4 was modeled using:

$$A_{exp} = A_i + (A_{f1} - A_i)F + K_2L_{mo}(A_{f2} - A_i)F + K_2L_{mo}K_3L_{mo}(A_{f3} - A_i)F$$

where $F = K_1L_{mo}/(1 + K_1L_{mo}(1 + K_2L_{mo}(1 + K_3L_{mo})))$, A_{f1}, A_{f2}, and A_{f3} are extinction coefficients for the three partly solvated species, K_1, K_2, and K_3 are the equilibrium constants, and L_{mo} is the concentration of monomeric methanol. In order to limit the number of degrees of freedom during simulation it was assumed that all bound species had the same extinction coefficient ±25%, as seems reasonable from the small to moderate deviations from isosbesticity observed. Over the concentration range of the titrations (0 to 0.2 M) a monomer−dimer−tetramer model was assumed for the oligomerization of methanol in CCl_4, using published values[23a] for the monomer−dimer equilibrium constant $K_{1,2} = 2.51$ and the dimer−tetramer equilibrium constant $K_{2,4} = 37.3$ (28 °C in CCl_4), and a value of −15 kJ/mol for the enthalpy of a methanol−methanol hydrogen bond[23c] in CCl_4, assuming one hydrogen bond in the dimer and four in the tetramer. L_{mo} was obtained from

$$4(K_{1,2})^2K_{2,4}(L_{mo})^4 + 2K_{1,2}(L_{mo})^2 + L_{mo} - L_o = 0$$

Here L_o is the total concentration of methanol. The observed UV equilibrium constant in wet or methanolic solvents, K_{obs}, was obtained by simulation of experimental data using the general expression for A_{exp} given above for 1:1 stoichiometry. For the equilibria in Figure 7:

$$F = (K_1L(1 + K_2L_2) + \beta)/(1 + K_1L(1 + K_2L_2) + \beta)$$

In this expression $L = L_o/(1 + \alpha)$, where L_o is the total concentration of added ligand as before, $\alpha = K_SL_2$ where K_S is the equilibrium constant for ligand solvation, L_2 is the total concentration of water or methanol, and $\beta = K_3L_2(1 + K_4L_2(1 + K_5L_2))$. When the K_5 term was not explicitly required in order to fit the data, as was the case in CH_2Cl_2 and $CHCl_3$, it was assumed that a third binding process was numerically subsumed in the K_4 term. Ligand solvation is modeled on the assumption that the ligand (polyol) can be considered as a collection of independent binding sites with an average per site interaction of K_S. From consideration of the above explicit expression for F it can be shown that $K_{obs} = K_1(1 + K_2L_2)/((1 + \alpha)(1 + \beta))$, eq 1 in the main text, with the corollary that the observed initial absorbance of the partly solvated receptor, A_{iobs}, is related to the absorbance in dry solvent by $A_{iobs} = A_i + (A_f - A_i)\beta/(1 + \beta)$. For equilibrium constants greater than 1×10^4 and 1:1 stoichiometry, UV titration data was fitted to $A_{exp} = A_i + \delta\epsilon C$, where $\delta\epsilon$ is the difference in extinction coefficients between free and bound receptor (porphyrin) at the wavelength of measurement and C is the concentration of complex satisfying the usual binding quadratic:

$$C^2 - (R_o + L_o + 1/K)C + R_oL_o = 0$$

where R_o is the total concentration of receptor. Observed equilibrium constants in wet or methanolic CCl_4 (K_{obs} between 10^5 and 10^7), were obtained by simulation of experimental data using the general expression for A_{exp} just given. It can be shown by expressing the above binding quadratic in terms of the total concentration of bound species that K_{obs} is again given by eq 1, and also that the observed absorbance and extinction coefficients parameters are related to the parameters in dry solvent by $A_{iobs} = A_i + \delta\epsilon R_o\beta/(1 + \beta)$ and $\delta\epsilon_{obs} = \delta\epsilon/(1 + \beta)$.

NMR data for 1:1 stoichiometry was fitted to $\delta_{obs,receptor} = \delta_o + (\delta_C - \delta_o)C/R_o$ for receptor resonances where δ_{obs} is the observed (averaged) chemical shift, δ_o is the chemical shift for free receptor, δ_C is the chemical shift for complex and C satisfies the binding quadratic above. NMR data for 1:2 (receptor/ligand) stoichiometry was fitted to

$$\delta_{obs,receptor} = \delta_o + ((\delta_{C_1} - \delta_o)C_1 + (\delta_{C_2} - \delta_o)C_2)/R_o$$

where δ_{C_1} and δ_{C_2} are the chemical shifts of complexes C_1 and C_2 respectively, and C_1 and C_2 satisfy the expressions:

$$(C_1)^3K_2(1 + 4K_2/K_1) + (C_1)^2(1 - 2K_2(R_o + 2/K_1)) - C_1(R_o + L_o + 1/K_1 + K_2L_o(L_o - 2R_o)) + R_oL_o = 0$$

and

$$C_2 = K_2C_1(L_o - C_1)/(1 + 2K_2C_1)$$

where K_1 and K_2 are the first and second equilibrium constants and L_o is the total ligand concentration. NMR data for 2:1 (receptor/ligand) stoichiometry was fitted to

$$\delta_{obs,receptor} = \delta_o + ((\delta_{C_1} - \delta_o)C_1 + 2(\delta_{C_2} - \delta_o)C_2)/R_o$$

with C_1 and C_2 satisfying the same expressions as above substituting L_o for R_o and *vice-verse*. The expressions for ligand resonances $\delta_{obs,ligand}$ are similar to those above. Least-squares curve fitting used the SIMPLEX algorithm[59] and binding polynomials were solved using published algorithms.[59]

Acknowledgment. We thank the SERC, Christ's College, and the Industrial Club of the Cambridge Centre for Molecular Recognition for financial support.

Supplementary Material Available: ^{1}H NMR spectrum of β-glucoside **5** in $CDCl_3$ showing concentration dependence of hydroxyl resonances, ^{1}H NMR spectrum of complex between **Zn1** and α-mannoside **4** in CCl_4, and UV titration data for **Zn1** and α-mannoside **4** in 0.05% v/v methanolic CCl_4 showing an isosbestic point (3 pages). This material is contained in many libraries on microfiche, immediately follows this article in the microfilm version of this journal, and can be ordered from the ACS; see any current masthead page for ordering information.

(59) Press, W. H.; Flannery, B. P.; Teukolsky, S. A.; Vetterling, W. T. *Numerical Recipes in Pascal: The Art of Scientific Computing*; Cambridge University Press: Cambridge, 1989.